Dissolved Inorganic Nutrients in the Western Mediterranean Sea (2004-2017)

Malek Belgacem[1,2], Jacopo Chiggiato[1,*], Mireno Borghini[1], Bruno Pavoni[2], Gabriella Cerrati[3], Francesco Acri[1], Stefano Cozzi[4], Alberto Ribotti[5], Marta Álvarez[6], Siv K. Lauvset[7], Katrin Schroeder[1]

[1] CNR-ISMAR, Arsenale Tesa 104, Castello 2737/F, 30122 Venezia, Italy

[2] Dipartimento di Scienze Ambientali Informatica e Statistica, Università Ca' Foscari Venezia, Campus Scientifico Mestre, Italy

[3] ENEA, Department of Sustainabiliy, S. Teresa, Marine Environmental center, 19032 Pozzuolo di Lerici (SP), Italy

[4] CNR-ISMAR, Area Science Park – Basovizza, 34149 Trieste, Italy

[5] CNR-IAS, Loc. Sa Mardini snc, Torregrande, 9170 Oristano, Italy

[6] Instituto Español de Oceanografía, IEO, A Coruña, Spain

[7] NORCE Norwegian Research Centre, Bjerknes Centre for Climate Research, 5007 Bergen, Norway

*Corresponding author's email: jacopo.chiggiato@ismar.cnr.it

Abstract

Long-term time-series are a fundamental prerequisite to understand and detect climate shifts and trends. Understanding the complex interplay of changing ocean variables and the biological implication for marine ecosystems requires extensive data collection for monitoring, hypothesis testing and validation of modelling products. In marginal seas, such as Mediterranean Sea, there are still monitoring gaps, both in time and in space. To contribute to filling these gaps, an extensive dataset of dissolved inorganic nutrients observations (nitrate, NO_3; phosphate, PO_4^{3-}; and silicate, SiO_2) have been collected between 2004 and 2017 in the Western Mediterranean Sea and subjected to rigorous quality control techniques to provide to the scientific community a publicly available, long-term, quality controlled, internally consistent biogeochemical data product. The data product includes 870 stations of dissolved inorganic nutrients, including temperature and salinity, sampled during 24 cruises. Details of the quality control (primary and secondary quality control) applied are reported.

The data are available in PANGAEA (https://doi.pangaea.de/10.1594/PANGAEA.904172, Belgacem et al. 2019)

Keywords: Mediterranean Sea, Dissolved Inorganic Nutrient, biogeochemistry

1 Introduction

Dissolved inorganic nutrients play a crucial role in marine ecosystem functioning. They serve as regulators of ocean biological productivity, and are trace elements for biogeochemical cycling as well as for natural and anthropogenic sources and transport processes (Bethoux, 1989; Bethoux et al., 1992). They are also non-conservative tracers, since their distribution vary according to both biological (such as primary production and respiration) and physical (such as convection, advection, mixing and diffusion) processes. Very schematically, inorganic nutrients are continuously consumed by phytoplankton (due to primary production) in the sea surface and regenerated in the mesopelagic layer by bacteria and animals (due to respiration). Moreover, the sinking of organic matter and its decomposition increases the nutrient concentrations in the intermediate and deep-water masses over time. To identify the limiting factors for biological production in the oceans, we need to understand the underlying chemical constraints and especially the macro- and micronutrients spatial and temporal variations. Dissolved inorganic nutrients may be used as tracers of water masses like salinity and temperature, to assess mixing processes, and to understand the biogeochemical circumstances of their formation regions. Understanding the complex interplay of changing ocean variables and the biological implication for marine ecosystems is a difficult task and requires not only modelling, but also extensive data collection for monitoring, hypothesis testing and validation. Monitoring gaps still remain in both in time and space, especially for marginal seas such as the Arctic Ocean or the Mediterranean Sea.

The Mediterranean Sea has been identified as a region significantly affected by ongoing climatic changes, like warming and decrease in precipitation (Giorgi, 2006). In addition, it is a region particularly valuable for climate change research because it behaves like a miniature ocean (Bethoux et al., 1999) with a well-defined overturning circulation characterized by spatial and temporal scales much shorter than for the global ocean, with a turnover of only several decades. Being an intercontinental sea, and subjected to more terrestrial nutrient inputs (river runoff, submarine groundwater discharge) and atmospheric deposition, the Mediterranean Sea has a nitrate to phosphate N:P ratio that is anomalously high compared to the “classical” world's oceans Redfield ratio, indicating a general P-limitation regime, which becomes stronger along a west-to-east gradient. The Mediterranean Sea is therefore a potential model to study global patterns that will be experienced in the next decades worldwide, not only regarding ocean circulation, but also the marine biota (Lejeusne et al., 2010). Several environmental variables can act as stressors for marine ecosystems, by which climatically driven ecosystem disturbances are generated (Boyd, 2011). These changes affect, among others, the distribution of biogeochemical elements (including inorganic nutrients) and the functioning of the biological pump and CO_2 regulation.

Within this context, the aim of this paper is to compile an extensive dataset of dissolved inorganic nutrient observations (nitrate, NO_3; phosphate, PO_4^{3-}; and silicate, SiO_2) collected between 2004 and 2017 in the Western Mediterranean Sea (WMED), to describe the quality control techniques and to provide the scientific community with a publicly available, long-term, quality controlled, and internally consistent biogeochemical data product, contributing to previously published Mediterranean Sea datasets like the MEDAR/Medatlas(time period:1908–1999), (Fichaut et al., 2003) and the Mediterranean Sea – Eutrophication and Ocean Acidification aggregated datasets v2018 (time period: 1911-2017) provided by EMODnet Chemistry (Giorgetti al.,2018) available at https://www.seadatanet.org/Products/Aggregated-datasets.

Both original and quality-controlled data are available in PANGAEA:

https://doi.pangaea.de/10.1594/PANGAEA.904172

Coverage: 44°N-35°S; -6°W-14°E

Location Name: Western Mediterranean Sea

Date start: May 2004

Date end: November 2017

2 Dissolved inorganic nutrient data collection

2.1. The CNR dissolved inorganic nutrient data in the WMED

Long-term time-series, such as the OceanSites global time series (www.oceansites.org), are a fundamental prerequisite to understand and detect climate shifts and trends. However, biogeochemical time-series are still limited to the northern western Mediterranean Sea (MOOSE network, Coppola et al., 2019) Yet, inorganic nutrients in the Mediterranean Sea has received more attention in recent years, and various datasets have been compiled to understand its unique characteristics such as the one build by the PERSEUS project Consortium ("Policy-oriented marine environmental research in the southern European seas" - EU FP7 project GA #287600), that included 100 cruises collected during the project's lifetime, in addition to those from other projects like SESAME, EU FP7 project GA #GOCE-036949), and data products such as the MEDAR/Medatlas. In addition to that, the data assembly system EMODnet Chemistry, a leading infrastructure supported by pan-European directorate General MARE set up (Martin Miguez et al., 2019, Tintoré et al.,2019).

The dataset presented here consists of 24 oceanographic cruises (Fig. 1 and Table 1) conducted in the WMED on board of research vessels run by the Italian National Research Council (CNR) and the Science and Technology Organisation Centre for Maritime Research and Experimentation (NATO-STO CMRE). All cruises were merged into a unified dataset with 870 nutrient stations and ~ 9666 data points over a period of 13 years (2004-2017). The overall spatial distribution of the stations covers the whole WMED, but the actual distribution strongly varies depending on the specific cruise and most of the data are collected along sections. At all stations, pressure, salinity and temperature were measured with a CTD-rosette system consisting of a CTD SBE 911 plus and a General Oceanics rosette with 24 12L Niskin Bottles. Temperature measurements were performed with the SBE-3/F thermometer with a resolution of 10^{-3} °C; conductivity measurements were performed with the SBE-4 sensor with a resolution of $3 \cdot 10^{-4}$ S/m. The probes were calibrated before and after each cruise. During all CNR cruises, redundant sensors were used for both temperature and salinity measurements.

Seawater samples for dissolved inorganic nutrient measurements were collected during the CTD up-cast at standard depths (with slight modifications according to the depth at which the deep chlorophyll maximum was detected). The standard depths are usually 5, 25, 50, 75, 100, 200, 300, 400, 500, 750, 1000, 1250, 1500, 1750, 2000, 2250, 2500, 2750, 3000 m. No filtration was employed, nutrient samples were immediately stored at −20 °C. Note that sample storage and freezing duration varied greatly from one cruise to another (Table 3 shows the cruises where this exceeded 1 year).

2.2. Analytical methods for inorganic nutrients

For all cruises, nutrient determination (nitrate, orthosilicate and orthophosphate) was carried out following standard colorimetric methods of seawater analysis, defined by Grasshoff et al. (1999) and Hansen and Koroleff (1999). For inorganic phosphate, the method is based on the reaction of the ions with an acidified molybdate reagent to yield a phosphomolybdate heteropoly acid, which is then reduced to a blue-colored compound (absorbance measured at 880 nm). Inorganic nitrate is reduced (with cadmium granules) to nitrite that react with an aromatic amine leading to the final formation of the azo dye (measured at 550 nm). Then, the nitrite separately determined must be subtracted from the total amount measured to get the nitrate concentration only. The determination of dissolved silicon is based on the formation of a yellow silicomolybdic acid reduced with ascorbic acid to blue-colored complex (measured at 820 nm).

Nutrient analysis was performed in three laboratories. From 2004 to 2013, all cruises nutrients were analysed by ENEA, while for those of 2015 (cruise #23) and 2017 (cruise #24), nutrient concentrations were analysed by CNR-ISMAR. Referring to Table 1S, four different models of autoanalyzer were used. Measurements from the autoanalyzer were reported in μmol L^{-1}. Inorganic nutrient concentrations were converted to the standard unit μmol kg^{-1}, using sample salinity from CTD and a mean laboratory analytical temperature of 20°C. Data from nutrient analysis were then merged to ancillary CTD bottle data.

2.3. Reference inorganic nutrient data

In addition to the data collected during the above-mentioned cruises, and in order to perform the secondary quality control (described below), we identified five reference cruises (Table 2), based on their spatial and temporal distribution of the data and the reliability of the measurements (see Fig. 2 – Table.3S Fig.1S). Cruises 06MT20110405 and 06MT20011018 are the only two Mediterranean cruises included in the publicly available Global Ocean Data Analysis Project version 2 (GLODAPv2, Olsen et al. 2016). These cruises, conducted on board the R/V Meteor, provide a reliable reference because nutrient analysis strictly followed the recommendation of the World Ocean circulation experiment (WOCE) and the GO-SHIP protocols (Hydes et al., 2010; ,Tanhua et al., 2013). Cruises 29AH20140426 and 48UR20070528 are to be included in the CARIMED data product (personal communication by M. Álvarez, in preparation but not yet available) and have undergone rigorous quality control following GLODAP routines. Finally, 29AJ20160818 was carried out in the framework of the MedSHIP programme (Schroeder et al., 2015) and its data are available at https://doi.org/10.1594/PANGAEA.902293 (Tanhua, 2019).

3 Quality Assurance and quality control methods

Combining inorganic nutrient data from different sources, collected by different operators, stored for different amounts of time, and analysed by multiple laboratories, is not a straightforward task. This is widely recognized in the biogeochemical oceanographic community. Since the 1990s, several studies and programmes (e.g. World Ocean Database, World Ocean Atlas, WOCE) have been devoted to facilitate the exchange of oceanographic data and develop quality control procedures to compile databases by the estimation of systematic errors (Gouretski and Jancke, 2001) to increase the inter-comparability, generate consistent data sets and accurately observe the long-term change.

An example of a first quality control procedure is the use of reference materials that are available for salinity (IAPSO, salinity standard by OSIL) and temperature (SPRT, Standard Platinum Resistance Thermometer). As for the inorganic carbon, total alkalinity (Dickson et al., 2003) and inorganic nutrients (Aoyama et al., 2016), certified reference materials (CRM) have been recently made applicable for oceanographic cruises. However, since CRM are not always available or used for biogeochemical oceanographic data, Lauvset and Tanhua (2015) developed a secondary quality control tool to identify biases in deep data. The method suggests adjustments that reduce cruise to cruise biases, increase accuracy and allow for the inter-comparison between data from various sources. This approach, based on a crossover and inversion method (Gouretski and Jancke, 2001; Johnson et al., 2001), was used to generate the CARbon IN Atlantic ocean (CARINA, see Hoppema et al., 2009), GLODAPv2.2019 (Olsen et al., 2019) and PACIFICA (Suzuki al al.,2013) databases.

3.1 Primary Quality control

Each individual cruise was first subjected to a primary quality control (1^{st} QC) that included a check of apparent and extreme outliers in CTD salinity, nitrate, phosphate and silicate. Each parameter included a quality control flag, following standard WOCE flags (Table 3). Surface, intermediate and deep layer were evaluated separately because nutrient observations evolve differently in each layer. The coefficient of variation (CV, defined as standard deviation over mean) was computed for each depth layer. Coefficients of variation in the surface (0-250 db) layer were high (nitrate CV=1.16, phosphate CV=1.005, silicate CV=0.75) due to air-sea interaction (Muniz et al., 2001) occurring in this layer rendering it difficult to flag. These influences are of reduced importance in the intermediate (250-1000 db) layer (nitrate CV=0.23, phosphate CV=0.31, silicate CV=0.24) and the deep (>1000 db) layer (nitrate CV=0.15, phosphate CV=0.22, silicate CV=0.14), decreasing the total variance. Flags in the upper and intermediate layer were thus set based on outliers within pressure ranges defined according to standard pressures (0-10, 10-30, 30-60, 60-80, 80-160, 160-260, 260-360, 360-460, 460-560, 560-1000 db).

Below 1000 db, flagging included an inspection of nitrate to phosphate (N:P) and nitrate to silicate (N: Si) ratios. The Median and Median Absolute Deviation (MAD) was computed by classes of pressure: we considered as outlier any atypical observation and any value that departs from the median by more than three MADs in the different pressure ranges for each cruise.

An overview of the nutrient distribution is provided with scatter plots, showing also the flagged measurements (Fig. 3). Each measurement was flagged 2 ("Acceptable/ measured") or flagged 3 ("Questionable"): 4.1% of nitrate data, 3.37% of phosphate data, 3.16% of silicate data, and 0.07% of CTD salinity data were considered outliers and flagged 3. As highlighted by Tanhua et al. (2010), the primary QC can be subjective depending on the expertise of the person flagging the data, thus flagging could bring in some uncertainties.

In order to have a first assessment of the precision of each cruise measurements, the standard deviation of observations deeper than 1000 db was calculated along with averages and standard deviations for each cruise and by subregions to have an overview about nutrient content variability in the deep layer and about the observations spatial spread of individual cruises (Table 4). Following the subdivision of Manca et al. (2004), the WMED has been divided into subregions (Fig.2S, Table 2S) according to the general circulation patterns (details in Manca et al.,2004). Table 4 displays the comparison of standard deviation of deep measurements for each cruise and within subregions. The overall standard deviation between cruises in the deep layer varied between 0.51 and 1.41 μmol kg^{-1} for nitrate, between 0.1 and 1.64 μmol kg^{-1} for silicate and between 0.025 and 0.078 μmol kg^{-1} for phosphate. Regional standard deviation of nitrate measurements below 1000 db varied between 0.08 μmol kg^{-1} in the Gulf of Lion (DF2) with cruise #9 and 1.6 μmol kg^{-1} in the Balearic Sea (DS2) observations of cruise #14.

Phosphate lowest regional standard deviation was 0.01 μmol kg^{-1} found in the observations of cruise #9 in Gulf of Lion (DF2), cruise #10 in Balearic Sea (DS2) and Algerian West (DS3), cruise #14 and cruise # 15 in Tyrrhenian South (DT3), cruise #18 in Algero-Provençal (DF1) and Sardinia Channel (DI1) while the highest standard deviation was 0.1 μmol kg^{-1} in the observations of cruise #12 in Algerian West (DS3). As for silicate, the lowest standard deviation was 0.02 μmol kg^{-1} observed in cruise #9 measurements of Gulf of Lion subregion (DF2) and the highest deep standard deviation was observed in cruise #6 in its all subregions together with cruise #5 measurement in Tyrrhenian North (DT1) with 1.83 μmol kg^{-1} standard deviation.

Cruises #3, #6 and #9 had the largest spatial extension (see right side of Fig. 9) with a high number of samples over more than seven subregions (Table 4) and the geographical variability of the distribution in dissolved inorganic nutrients results thus in the largest standard deviations. Conversely, cruises with smaller spatial coverages have lower standard deviations. Therefore, a relatively small spatial coverage and high standard deviation is considered as indicative of data with low precision (Olsen et al., 2016). This applies to cruises #1, #5, and #16. Despite the small spatial coverage, samples of nitrate and phosphate of cruise #5 have an overall standard deviation of 1.35 μmol kg^{-1} and 0.07 μmol kg^{-1}, respectively, a high standard deviation pointed out in also in the regional standard deviation of deep measurements in Tyrrhenian North (DT1) and South (DT3) . Cruise #1, with few stations in Tyrrhenian North (DT1) and South (DT3) subregions and 21 samples below 1000 db, has an overall standard deviation of 1.25 μmol kg^{-1} for nitrate, 0.06 μmol kg^{-1} for phosphate and 1.64 μmol kg^{-1} for silicate. The regional standard deviation was relatively high for nitrate (0.51-1.32μmol kg^{-1}) phosphate (0.02-0.065μmol kg^{-1}) and silicate (0.53-1.83μmol kg^{-1}). A comparison with the deviations from e.g. cruise # 2, carried out in the same year and e.g. cruise #17 (with a similar cruise track), confirms the lower precision of the data of cruise#1. Similar considerations apply to the quality of nitrate samples (0.87-1.02 μmol kg^{-1}).and silicate (0.87-0.9 μmol kg^{-1}) from cruise #16, covering a small area in

Tyrrhenian North (DT1) and South (DT3), compared to cruise #17, carried out in the same regions (right side of Fig. 9 and Table 4).

Deep silicate measurements of cruise #6 have twice the overall standard deviation of silicate data of cruise #8 from the same year. Adding to that, in the seven subregions, the regional standard deviation of deep silicate observations was the highest, between 1.04-2 μmol kg^{-1} which was relatively high compared to the surrounding cruises that have observations in the same subregions. This is again suggestive of the limited precision. On the other hand, trying to explain the source of relatively high standard deviations in specific cruises is not always straightforward, as they could stem from a variety of sources, sampling, conservation and analysis. The bottom water in the WMED exhibits a high nutrient content below 1000 db (Table 4), due to the longer residence time. Dividing the WMED into subregions, has effectively removed the natural spatial change in nutrients, making the interpretation of the standard deviation a matter of the precision of the measurements only.

In Table 4, deep averages by subregions showed that overall nutrient fluctuated around 7.4 ±0.9μmol kg^{-1} for nitrate, 0.3 ±0.06 μmol kg^{-1} for phosphate and 7.7 ±0.8μmol kg^{-1} for silicate, similar findings were reported by Manca et al. (2004). Comparing cruise averages in each region enabled the identification of “suspect” cruises. Cruise #24 has the lowest deep average in nitrate in Algéro-Provençal (DF1), Tyrrhenian North (DT1) subregions and Sardinia Channel (DI1). As for silicate of cruises #24 and #16 was very low compared to the overall regional average in Liguro-Provençal (DF3) and Tyrrhenian South (DT3) subregions. Deep average of phosphate did not show any outlier cruises in all subregions. Different reasons could explain the low precision in the samples, freezing is one. Although it is a valid preservation method (Dore at al.,1995), the error is higher when samples were not analysed immediately (Segura-Noguera et al., 2011), so the storage time could influence.

3.2 Secondary Quality control: the crossover analysis

The method used to perform the secondary QC on the dissolved inorganic nutrient dataset in the WMED makes use of the quality-controlled reference data, and the crossover analysis toolbox developed by Tanhua (2010) and Lauvset and Tanhua (2015). The computational approach is based on comparing the cruise data set to a high-quality reference data set to quantify biases, described in detail in Tanhua et al. (2010). Here, we summarize the technique with emphasis on inorganic nutrient. The first step consisted of selecting reference data, as described in section 2.3. The second step is the crossover analysis that was carried out using a MATLAB Toolbox (available online: https://cdiac.ess-dive.lbl.gov/ftp/oceans/2nd_QC_Tool_V2/) where crossovers are generated as difference between two cruises using the "running cluster" crossover routine. Each cruise is thus compared to the chosen set of reference cruises. For each crossover, samples deeper than 1000 db are selected within a predefined maximum distance set to 2°arc distance, defined as a crossing region, to ensure the quality of the offset with a minimum number of crossovers and to minimize the effect of the spatial change. The reason to select measurements deeper than 1000 db, is to remove the high frequency variability associated to mesoscale features, biological activity and the atmospheric forcing acting in the upper layers, that might induce changes in biogeochemical properties of water masses. On the other hand, also the deep Mediterranean cannot be considered truly "unaffected" by changes, as it is intermittently subjected to ventilation (Schroeder et al., 2016; Testor et al., 2018) and the real variability can be altered in adjusting data. The computational approach takes this into account, since weights are given to the less variant profile in the crossing region, according to the "confidence" in the determined offset of the compared profiles (i.e. the weighted mean offset of a given crossover-pair is weighted to the depth where the offsets of all compared profiles have the smallest variation (which indeed is strongly interlinked with the degree of variance of each profile) (for further details see Lauvset and Tanhua, 2015).

Before identifying crossovers, each profile was interpolated using the piecewise cubic Hermite method and the distance criteria outlined in Lauvset and Tanhua (2015), their Table 1, and detailed in Key et al. (2004). The crossover is a comparison between each interpolated profile of the cruise being evaluated and the interpolated profile of the reference cruise. The result is a weighted offset (defined as difference cruise/reference) and a standard deviation of the offset. The standard deviation is indicative of the precision; however, it is important to note that this assumption only works because it is a comparison to a reference, and the absolute offset is indicative of accuracy.

The third step consists in evaluating and selecting the suggested correction factor that was applied to the whole water column. The correction factor was calculated from the weighted mean offset of all crossovers found between the cruise and the reference data set, involving a somewhat subjective process.

For inorganic nutrients, offsets are multiplicative so that a weighted mean offset > 1 means that the measurements of the corresponding cruise are higher than the measurements of the reference cruise in the crossing region and applying the adjustment would decrease the measured values. The magnitude of an increase or a decrease is the difference of the weighted offset from 1. In general, no adjustment smaller than 2% (accuracy limit for nutrient measurements) is applied (detailed description is found in Hoppema et al., 2009; Lauvset and Tanhua, 2015; Olsen et al., 2016; Sabine et al., 2010; Tanhua et al., 2010).

The last step is the computation of the weighted mean (WM) to determine the internal consistency and quantify the overall accuracy of the adjusted product (Hoppema et al., 2009; Sabine et al., 2010; Tanhua et al., 2009), with the difference that our assessment is based on the offsets with respect to a set of reference cruises. This WM reflects the absolute weighted mean offset of the data set compared to the reference data set, hence the smaller the WM the higher the internal consistency. The accuracy was computed from the individual absolute weighted offsets. The WM, which will be discussed in section 4.4., was computed using the individual weighted absolute offset (D) of number of crossovers (L) and the standard deviation (σ): $\mathrm{WM}=\frac{\sum_{i=1}^{L} D(i)/(\sigma(i))^2}{\sum_{i=1}^{L} 1/(\sigma(i))^2}$

4 Results of the secondary QC and recommendations

The results of the secondary QC revealed the necessary corrections for nitrate, phosphate and silicate. Four cruises were not considered in the crossover analysis: cruises #7 and #11 do not have enough stations > 1000 db (at least 3 to get valid statistics), while cruises#19 and #21 were outside the spatial coverage of the reference cruises. Cruises that were not used for the crossover analysis are made available in the original dataset but were not included in the final data product (see Supplementary material – Part 2 (A2)).

Overall, we found a total number of 73 individual crossovers for nitrate, 72 for phosphate and 54 for silicate. An example of the running cluster crossover output is shown in Fig.4. Results of the crossover analysis is an adjustment factor for each cruise and each nutrient, that are shown in Table 5 and Fig. 5-6-7. The adjustment factor was calculated from the weighted mean of absolute offset summarized in Table 6 and Fig. 3S-4S-5S. Table 6 details the improvement of the weighted mean of absolute offset by cruise prior to and after adjustments, the information is also displayed graphically in Fig. 3S-4S-5S. Cruises are in chronological order in all figures and tables.

4.1 Nitrate

The crossover analysis suggests a significant adjustment for nitrate concentrations on 15 cruises, between 0.94 and 0.98 (for adjustments <1) and between 1.02 and 1.34 (for adjustments >1) (Table 5 and Fig.5). Offsets suggest that the deep measurements of cruises #1, #3, #4, #5, #6, #8, #12, #13, #15, #16, #23 and #24 need to be adjusted towards higher concentrations, when compared to the respective reference (Fig.3S).

Nitrate observations of cruises #2, #9 and #10 on the other hand were higher than the reference cruises and exhibit variation outside the accepted accuracy limit, thus requires a downward adjustment.

Finally, five cruises (#14, #17, #18, #20, and #22) were consistent with the reference data and no adjustment was necessary. Considering the weighted mean of absolute offset after adjustments shown in Table 6, two cruises (#5 and #24) required large correction factors but still remain outside the accuracy threshold (Fig. 5). These cruises are considered in detail later (section 4.4).

4.2 Phosphate

For phosphate the crossover analysis suggests adjustments for 20 cruises, as shown in Fig. 6. Deep phosphate measurements of 15 cruises (Table 6) appear to be lower than the respective reference measurements (i.e. phosphate data of these cruises require an upward adjustment), while the data of five cruises (#2, #3, #4, #6, #24) are higher (i.e. they need a downward adjustment) (Fig.4S). Applying all the indicated adjustments, the large offsets of cruises #2, #3, #4, #6, #8, #9, #10, #18, #20, #23 and #24 are reduced and become consistent with the reference. Cruises #1, #5, #12, #13, #14, #15, #16, #17, and #22 retain an offset even after applying the indicated adjustment. These cruises are considered in detail later.

According to Olsen et al. (2016), if a temporal trend is detected in the offsets, no adjustments should be applied. There is indeed a decreasing trend between 2008 and 2017 in the phosphate correction factor (Fig. 6), and thus an increasing one in the weighted mean offset (Fig.4S), implying a temporal increase of phosphate. Therefore, phosphate data of the cruises being part of the trend were not flagged as questionable, except some cruises that are discussed further in section 4.4.

Comparing phosphate before and after adjustments, the corrections did minimise the difference with the reference, while the actual variation with time was preserved (Fig.6). The temporal trend towards higher phosphate concentrations in the Mediterranean Sea is considered to be real, even though studies concerning the biogeochemical trends in the deep layers of the WMED are scarce (Pasqueron et al., 2015). However, this variation could be consistent with the findings of Béthoux et al.(1998, 2002) and the modelling studies by Moon et al. (2016) and Powley et al. (2018) who indeed found an increasing trend in phosphate concentrations over time, due to the increase in the atmospheric and terrestrial inputs.

4.3 Silicate

The results of the crossover analysis for silicate suggests corrections for all cruises (Fig.7). The crossovers indicate that deep silicate measurements are lower in the evaluated cruises than in the corresponding reference cruises (i.e. they need to be adjusted upward) (Fig.5S). This is likely to be a direct result of freezing the samples before analysis, since the reactive silica polymerizes when frozen (Becker et al., 2019). After applying the adjustment (Table 5), as expected, the offsets are reduced (Table 6), but five cruises (#1, #5, #6, #15, and #16) remain outside the accuracy envelope. Due to the large offsets, these cruises will be discussed further in section 4.4.

4.4 Discussion and recommendation

Adjustments were evaluated for each cruise separately. As a general rule no correction was applied when the suggested adjustment is strictly within the 2% limit (indicated with NA in Table 5). The average correction factors were 1.06 for nitrate, 1.14 for phosphate and 1.14 for silicate, respectively. To verify the results, we re-ran the crossover analysis and re-computed offsets and adjustment factors using the adjusted data (as shown in blue in Fig. 3S-4S-5S and Fig. 5-6-7). Most of the new adjustments are within the accuracy envelope and few are outside the limit, except for the cruises belonging to the above mentioned "phosphate-trend" and the other outlying cruises which are detailed hereafter. By the application of adjustments, the deep-water offsets were reduced. This can be seen in the decrease of the weighted mean offset between the data before adjustments (after 1st QC, Fig. 3S-4S-5S, in grey) and the adjusted data (after 2nd QC, Fig. 3S-4S-5S, in blue).

Referring to the analysis detailed in section 3.2, the internal consistency of the nutrient data set has improved and increased significantly after the adjustment, from 4% for nitrate, 19% for phosphate and 13% for silicate, to a more unified dataset with 3 % for nitrate, 6 % for phosphate and 3% for silicate.

A comparison between the original and the adjusted nutrient observations is shown in Fig. 8A-B-C, indicating an improvement in the accuracy based on the reference measurement and a relatively reduced range particularly for phosphate (Fig. 8B). Figure 8. D-E scatterplots show that after the quality control, nutrient stoichiometry slopes obtained from regressions, between tracers along the water column show a strong coupling and provide a nitrate to phosphate ratio of ~22.09 and a nitrate to silicate ratio of ~0.94. These values are consistent with nutrient ratios range found in the WMED as reported in Lazzari et al. (2016); Pujo-Pay et al., (2011) and Segura-Noguera et al. (2016).

The regression model is more accurate after adjustments with an improved r^2 for N:P (from 0.81 to 0.90) and for N: Si (from 0.85 to 0.87). One of the main reasons for an upward/ downward bias would be the lack of use of CRM for nutrients in all cruises as also noted in CARINA (Tanhua et al., 2009) or in the most recent global comparability study by Aoyama (2020).

In the following some details on the adjustment of specific cruises are given:

Cruise #2 [48UR20041006] needed an adjustment of 0.98 for nitrate, 0.9 for phosphate and 1.06 for silicate. Most of the crossover profiles occur in the Tyrrhenian sea (Tyrrhenian North and Tyrrhenian South subregions). After adjustment, the cruise is inside the 2% envelope.

Cruise #3 [48UR20050412] appeared to be outside the 2% envelope before adjustments. Its offsets with five reference cruises, crossing the Tyrrhenian sea, Sardinia channel, Gulf of Lion and Algero-Provençal subregions, showed that nitrate and silicate values to be relatively low, and thus an adjustment of 1.08 and 1.15 was applied respectively. On the other hand, phosphate values were relatively high, and a 0.93 adjustment was applied.

Cruise #4 [48UR20050529] correction factor estimate was based on five crossovers that covered five subregions: Tyrrhenian South, Sardinian channel, Algerian East and West and the Alboran sea. Table 4) show that there are no large differences between regional averages within the cruise which justify an adjustment of 1.04 for nitrate, 0.85 for phosphate and 1.183 for silicate.

Cruise #8 [48UR20060928] was adjusted by 1.03 for nitrate, 1.14 for phosphate and 1.1 for silicate, because it showed values to be low compared to four references. After adjustment, the data were inside the acceptable range.

Cruise #9 [48UR20071005] values of nitrate were slightly outside the 2% envelope before adjustments, similar to phosphate and silicate that were lower compared to the reference. The adjustments of 0.97 for nitrate, 1.14 for phosphate and 1.115 for silicate suggested by the mean offset against the reference cruises were recommended.

Cruise #13 [48UR20090508] has three crossovers in the common crossing zone that included Tyrrhenian North, Tyrrhenian South and Sardinia Channel subregions. The crossover suggests that this cruise has too low values and needs an adjustment of 1.05 for nitrate, 1.33 for phosphate and 1.15 for silicate.

Cruise #14 [48UR20100430] has a mean offset with four reference cruises that suggests an adjustment for phosphate of 1.34 and silicate of 1.123. Nitrate did fall within the accuracy envelope.

Cruise #10 [48UR20080318] has only three crossovers in the Algero-Provençal subregion, showing that nitrate is too high compared to the reference while phosphate and silicate are slightly lower. We therefore applied the adjustments of Table 5, since the deep averages for each region (table 4) did not show large regional difference.

Cruise #17 [48UR20110421] crossover analysis did not suggest any correction for nitrate, However, for phosphate and silicate with an offset based on two crossovers in the Tyrrhenian North and South subregions, adjustments were recommended for phosphate (1.25) and silicate (1.12), for being lower than the reference cruises.

Cruise #18 [48UR20111109] is similar to cruise #17, since it was suggested to correct phosphate by 1.14 and silicate by 1.09, based on four crossovers in the Tyrrhenian North and South, Sardinia channel and Algero-Provençal subregions.

Cruise #20 [48UR20120111] has four crossovers over the Tyrrhenian North and South and Algero-Provençal subregions. Its measurements were slightly lower than the reference cruises suggesting a correction factor of 1.17 for phosphate and 1.08 for silicate.

Cruise #22 [48UR20131015] has similar correction factors as cruise#20, based on three crossovers in the Sardinia channel and Tyrrhenian North and South subregion, with measurements being lower than the reference.

Cruise #23 [48QL20150804] showed nutrient values slightly lower than the reference cruises as well, suggesting small correction factors of 1.02 for both nitrate and phosphate and 1.08 for silicate that were based on offsets with five cruises.

Below, we discuss the recommended flags in the final product (Table 3) assigned for some cruises that needed further consideration, since they required larger adjustment factors:

Cruise #1 [48UR20040526]: The adjusted values are still lower than the reference (Fig.5-6-7-Fig.3S-4S-5S) and are still outside the 2% accuracy range. This cruise had stations in the Sicily Strait, Tyrrhenian North and South and Ligurian East sub-regions. (Fig. 9, right side) and only 4 stations were deeper than 1000 db (those within the Tyrrhenian Sea). The low precision of this cruise has already been evidenced during the primary QC (section 3.1). We recommend flagging this cruise as questionable (flag 3).

Cruise #5 [48UR20051116]: This cruise took place between Sicily Strait and the Tyrrhenian North and South (Fig. 9, right side). Nitrate, phosphate and silicate data were lower than those from other cruises (#3 and #4) run the same year (Fig. 5-6-7-Fig.3S-4S-5S) and are still biased after adjustments.

Considering the limited precision and the low number of crossovers, it is recommended to flag the cruise as questionable (flag 3).

Cruise #6 [48UR20060608]: This cruise had an offset with five cruises giving evidence that adjustments of 1.05 for nitrate, 0.86 for phosphate and 1.26 for silicate are needed. The silicate bias was reduced after adjustment but remains large with respect to the accuracy limit (Fig. 7-Fig. 5S). This cruise has a wide geographic coverage, with stations along 9 sections (Fig. 9, right side). Considering also the high standard deviation (Table 4), which is partially attributed to the spatial coverage of the cruise, there is still uncertainty about the quality of the samples. It is recommended to flag silicate data of cruise #6 as questionable (flag 3).

Cruise #12 [48UR20081103]: Phosphate data have low accuracy with respect to the reference cruises (Fig. 6-Fig. 4S). This cruise has stations along a longitudinal section from the Sicily Strait to the Alboran Sea, which might explain the large standard deviation of deep phosphate samples (Table 4). Cruise #12 was given a correction of 1.08 for nitrate, 1.12 for silicate and 1.38 for phosphate. The mean offset from five crossovers computed within the Tyrrhenian South, Sardinia Channel, Algerian East, Algerian West and Alboran Sea subregions suggests that this cruise has lower nutrient values than the reference cruise. After adjustment, cruise #12 is within the acceptable range for nitrate and silicate but not for phosphate as highlighted in section 3.2. In addition, considering the relatively high number of stations >1000 db and a plausible trend in phosphate, it is recommended to flag the phosphate data as good/acceptable.

Cruise #15 [48UR20100731]: This cruise had 149 station along a similar track as cruise #12but shows larger offsets for phosphate and silicate (Fig. 6-7-Fig. 4S-5S), compared to cruise #12. Considering that deep silicate data was not of low quality (small standard deviation, see Table 4), and that deep phosphate fall within the “phosphate-trend” discussed above, these data are flagged good/acceptable.

Cruise #16 [48UR20101123]: The cruise shows large offsets for phosphate and silicate (Fig. 6-7- Fig. 4S-5S), similar to cruise #15. Considering that the overall cruise standard deviation of silicate samples below 1000 db was relatively high (1.02 over 14 samples, see Table 4), and that it has only one crossover between the Tyrrhenian North and South subregions (Table 6), and that when comparing deep regional averages, this cruise had the lowest average silicate value, it is recommended to flag silicate data of cruise #16 as questionable (flag 3). As for phosphate, the cruise is part of the "phosphate-trend" and is therefore flagged good/acceptable e.

Cruise #24 [48QL20171023]: This cruise has the largest offset for nitrate even after adjustment. It is very likely due to a difference between laboratories (calibration standards) concerning nitrate, which needs to be flagged as questionable in the final product.

The cruises discussed in this section were not removed from the final product but are retained along with their recommended quality flag (Table 3) detailed above and in the supplementary material – Part 2 (A2)). We have done the evaluation of their overall quality but leave it up to the users how to appropriately use these data.

4.5 Product assessment: Comparison with MEDATLAS

Averages water mass properties have been computed from the adjusted product (Table 7), and compared to the MEDAR/Medatlas annual climatological profiles, downloaded from the Italian NODC website (http://doga.ogs.trieste.it/medar/) given by Manca et al. (2004), in order to evaluate and asses the new product. Since nutrient properties exhibit differences with depths, we compared average nutrient concentrations of the three main water masses in twelve subregions of the WMED (Table 7, Fig 2S).

The results of Table 7 compares water mass biogeochemical properties with the reference climatology. The new product agrees well with the Medatlas climatology. However, there are some distinctions. The surface layer (0-150db) is characterized by a low nutrient content. The surface nitrate varies between 0.69 and 2.75 μmol kg^{-1} with a maximum found in the Ligurian East (DF4) and the minimum in the Alboran Sea (DS1) subregions, similar values were recorded in the climatology (0.61- 3.00

μmol kg^{-1}). The differences in nitrate averages in the surface layer are observed in the Gulf of Lion (DF2) where the new product is higher than the climatology and slightly lower in the Liguro-Provençal (DF3). As for, the surface content in phosphate, it varied between 0.04 and 0.16 μmol kg^{-1} with a maximum found in the Ligurian East (DF1) and a minimum in the Alboran Sea (DS1), alike the Medatlas climatology, where phosphate averages fluctuate between 0.05 and 0.19 μmol kg^{-1} .The new product is slightly lower compared to the climatology. As to the average surface in silicate, it varies between 1.36 and 2.91 μmol kg^{-1} with a minimum found in the Ligurian East (DF4), the maximum in the Gulf of Lion (DF2)) while in the climatology it varied between 1.27 and 2.31 μmol kg^{-1} (the minimum in the Ligurian East (DF4) and the maximum in the Alboran Sea (DS1)). The new product is slightly higher in silicate.

Overall, the differences in the surface layer are observed in Gulf of Lion (DF2), Liguro-Provençal (DF3), Ligurian East (DF4), which is due to the intense variability of the vertical mixing occurring in the northern WMED compared to the other regions.

In the intermediate layer, averages were computed from the depth of the salinity maximum (S_{max}) ±100m from a regional average profile, indicative of the Levantine Intermediate Water (LIW) core. Nitrate average varies between 4.94 and 9.32 μmol kg^{-1} where the minimum content is recorded in Sicily strait (DI3) and the maximum in the Algerian West (DS3) while in the in the Medatlas climatology nitrate was between 5.14 and 8.60 μmol kg^{-1} . In average, the lowest content in nitrate was in Tyrrhenian North (DT1), South (DT3), Sardinia Channel (DI1) and Sicily Strait (DI3) while LIW of Gulf of Lion (DF2), Liguro-Provençal (DF3), Ligurian East (DF4), Balearic Sea (DS2), Algero-Provençal (DF1), Alboran Sea (DS1), Algerian West (DS3) and East (DS4) subregions is relatively rich in nitrate. Compared to the Medatlas product, though the new product is slightly higher mainly in the Gulf of Lion (DF2), Ligurian East (DF4) and Balearic Sea (DS2). As for phosphate, LIW averages show similar behavior as nitrate, the lowest phosphate content (0.21- 0.27 μmol kg^{-1}) is observed in the Eastern subregions of WMED (Sicily Strait (DI3),Sardinia Channel (DI1), Tyrrhenian South (DT3) and North (DT1), when the maximum concentrations (0.4-0.37 μmol kg^{-1}) were reported in the Western subregions of the WMED (the Alboran Sea (DS1), Algerian West (DS3) and East (DS4), Balearic Sea (DS2) and Gulf of Lion (DF2)). The large differences between the two products were in Ligurian East (DF4) and the Alboran Sea (DS1), subregions of few number of observations.

Concerning silicate, the lowest average concentration (5.25 μmol kg^{-1}) is observed in LIW core of the Sicily Strait (DI3,) and the maximum concentrations (8.66 - 8.77 μmol kg^{-1}) are in Alboran Sea (DS1) and Gulf of Lion (DF2), similar values were recorded in the Medatlas climatology (4.86-7.95 μmol kg^{-1}). There are some discrepancies, where the new product is higher particularly in the Gulf of Lion (DF2), Liguro-Provençal (DF3) and Algerian West (DS3) subregions. This difference is explained by the limited number of observations within depth range in the new product compared to the observations used in the climatology in these subregions.

Referring to Manca et al.,(2004), the LIW core salinity values are relatively more pronounced in Sicily strait (DI3), Sardinia channel (DI1) and in the Tyrrhenian South (DT3), North (DT1) subregions, where nutrients were lower than the Western subregions (DS3,DS4, DS1 , DF1, DS2, DF4, DF3, DF2). The averages of nutrient within the LIW core ties well with the Medatlas climatology averages (Table 7), except in subregions with important vertical mixing.

We have verified also average biochemical properties in the deep layer (below 1500db). The new product is slightly higher in nitrate averages (7.74 -8.37 μmol kg^{-1}) than the Medatlas climatology (7.12 - 8.06 μmol kg^{-1}) (Table 7). The largest difference is found in Tyrrhenian South (DT3) and North (DT1) subregions. This difference could be due to the fact that, we are comparing two different time periods (2004-2017 and 1908-2001). As for the deep layer phosphate, average concentrations vary between 0.35 and 0.37 μmol kg^{-1} and are within the climatology limits (0.31 - 0.40 μmol kg^{-1}). In all subregions, there is not large differences. Overall, phosphate is in accordance with the Medatlas climatology. Similar to nitrate, deep average silicate in the new product (8.64 -9.21 μmol kg^{-1}) is higher than the climatology (7.51 to 9.04 μmol kg^{-1}). The largest difference in average silicate is observed in Tyrrhenian North (DT1), South (DT3) and Liguro-Provençal (DF3) subregions.

We then used the Root Mean Squared Error (RMSE) as statistical index to quantify the difference between averaged regional profiles from the new products and Medatlas product. The climatology annual profiles were interpolated to the regional average profiles of the new product, and the average RMSE for each layer and subregion was calculated. Fig. 10 shows the regional evolution of RMSE in the main water masses for the three nutrients. For nitrate (Fig. 10 A), the RMSE vary between 0.12 μmol kg^{-1} in Tyrrhenian North (DT1) and 1.36 μmol kg^{-1} Gulf of Lion (DF2) in the surface layer, between 0.07 μmol kg^{-1} in the Sardinia Channel (DI1) and 2.35 μmol kg^{-1} in Gulf of Lion (DF2) in the intermediate layer, and between 0.11 μmol kg^{-1} Algerian East (DS4) and 0.79 μmol kg^{-1} Gulf of Lion (DF2). The RMSE decreases in the Algerian East (DS4), Tyrrhenian North (DT1), Tyrrhenian South (DT3), Sardinia Channel (DI1) and Sicily Strait (DI3). This illustrates the low difference between the two products.

For phosphate (Fig. 10 B), the RMSE ranges between 0.0022 μmol kg^{-1} in the Tyrrhenian South (DT3) and 0.12 μmol kg^{-1} in the Ligurian East (DF4) in the surface layer, and between 0.003 μmol kg^{-1} in the Liguro-Provençal subregion (DF3) and 0.048 μmol kg^{-1} in the Alboran Sea (DS1), while in the deep layer RMSE varied between 0.0087 in the Gulf of Lion (DF2) and 0.057 μmol kg^{-1} in the Tyrrhenian North (DT1).

Silicate RMSE (Fig. 10 C) is between 0.13 μmol kg^{-1} in the Algero-Provençal subregion (DF1) and 3.5 μmol kg^{-1} in the Ligurian East subregion (DF4) in the surface layer, between 0.10 μmol kg^{-1} in the Sardinia Channel (DI1) and 2.54 μmol kg^{-1} in the Gulf of Lion (DF2) in the intermediate layer, and in deep layer, RMSE ranges between 0.33 μmol kg^{-1} in the Algerian East (DS4) and 1.43 μmol kg^{-1} in the Liguro-Provençal subregion (DF3).

The best agreement between the two products was observed in the intermediate and deep layer. The lowest RMSE was confined to the deep layer in most of the subregions while the highest difference was found in the surface layer since it is subjected to intense vertical mixing mainly in the northern WMED. Comparing averages in subregions, showed similar differences in nutrient between the two products particularly in the Gulf of Lion (DF2), the Liguro-Provençal (DF3), Ligurian East (DF4) and Algerian East (DS4), due to the relative high variability in nutrient concentrations in these subregions. These differences are not significant as there is discrepancy on the number of observations used in the two products. Overall, inorganic nutrients of the new product agree very well with the MEDAR/Medatlas climatology. The main features of the spatial distribution in the inorganic nutrients were in accordance with the findings of Manca et al., (2004), where the relative high content in nutrient was found in the intermediate layer of the Algerian subregions (DF1, DS3, DS4) than in other subregions (table 7). Besides, the highest concentrations in deep layer silicate were reported in the Algerian subregions (9.21 μmol kg^{-1} (DS3) in the new product; 9.04 μmol kg^{-1} (DS4) in the climatology) in the two products, which is indicative of the poor regional ventilation and of the longer residence time of deep water especially in these subregions.

5 Final remarks

An internally consistent data set of dissolved inorganic nutrients has been generated for the WMED (2004-2017). The accuracy envelope for nitrate and silicate was set to 2%, a predefined limit used in GLODAP and CARINA data products. Regarding phosphate data, these were almost entirely outside this limit, because of its natural variations and overall very low concentrations in the WMED, a highly P-limited basin. Using a crossover analysis (2nd QC toolbox) to compare cruises with respect to reliable reference data, improved the accuracy of the measurements by bias-minimizing the individual cruisesthe new product was broadly in consistent with the earlier climatology MEDAR/Medatlas.

The publication of a quality-controlled extensive (spatially and temporally) database of inorganic nutrients in the WMED was timely and fills a gap in information that prevented baseline assessments on spatial and temporal variability of biogeochemical tracers in the Mediterranean. In combination with older databases in the same region (e.g. bottle data available in the MEDAR/Medatlas database), this new database will thus constitute a pillar on which the Mediterranean marine scientific community will be able to build on original research topics on biogeochemical fluxes and cycles and their relation to hydrological changes that occurred in the period covered by the dataset. The dataset is also relevant for the modelling community as it can be used as an independent data product to assess reanalysis products or it can be assimilated in new reanalysis products.

6 Data availability

The final product is available as a .csv merged file from PANGAEA, and can be accessed at https://doi.pangaea.de/10.1594/PANGAEA.904172 (Belgacem et al. 2019).

Ancillary information is in the supplementary materials with the list of variables included in original and final product. Table 1 summarizes all cruises included in the dataset. The dataset include frequently measured stations and key transects of the WMED with in situ physical and chemical oceanographic observations. As mentioned, two files are accessible, both include oceanographic variables observed at the standard depths (see supplementary Materials Part-2).

- *Original dataset: CNR_DIN_WMED_20042017_original.csv:* This is the original dataset with flag variable for each of the following parameter: CTD salinity, nitrate, phosphate and silicate from the primary quality control (detailed in section 3.1).
- *Adjusted dataset: CNR_DIN_WMED_20042017_adjusted.csv*: This is the product after primary quality control and after applying the adjustment factors from the secondary quality control. Recommendations of section 4.4 are included, as well as quality flags.

Author contribution: MB, MA, SL, JC and KS substantially contributed to write the manuscript. SC, GC and FA run the chemical analysis and contributed to the manuscript. MB coordinated the technical aspects of most of the cruises. SC, GC, FA, AR, BP contributed in specific part of the manuscript.

Acknowledgements. The data have been collected in the framework of several of national and European projects, e.g.: KM3NeT, EU GA #011937; SESAME, EU GA #GOCE-036949; PERSEUS, EU GA #287600; OCEAN-CERTAIN, EU GA #603773; COMMON SENSE, EU GA #228344; EUROFLEETS, EU GA #228344; EUROFLEETS2, EU GA # 312762; JERICO, EU GA #262584; the Italian PRIN 2007 program "Tyrrhenian Seamounts ecosystems", and the Italian RITMARE Flagship Project, both funded by the Italian Ministry of University and Research. We thank Sarah Jutterström from the Swedish Environmental Research institute for the invaluable help in Quality Control discussions. We would like to express our appreciation to the INOCEN laboratory team at IEO for their help and collaboration during MB's stay there. The authors are deeply indebted to all investigators and analysts who contributed to data collection at sea during so many years, as well as to the PIs of the cruises (S. Aliani, M. Astraldi, M. Azzaro, M. Dibitetto, G. P. Gasparini, A. Griffa, J. Haun, L. Jullion, G. La Spada, E. Manini, A. Perilli, C. Santinelli, S. Sparnocchia), the captains and the crews for allowing the collection of this enormous dataset; without them, this work would not have been possible.

References

Aoyama, M., Woodward, E. Malcolm S. Bakker, K., Becker, S., Björkman, K., Daniel, A., Mahaffey, C., Murata, A., Naik, H., Tanhua, T., Rho, T., Roman, R. and Sloyan, B.: Comparability of oceanic nutrient data. Poster Cluster Community Whitepaper, CLIVAR Open Science Conference on "Charting the course for climate and ocean research", 18-25 September 2016, Qingdao (China), 12 pp, http://hdl.handle.net/10261/17137, 2016.

Aoyama, Michio.: Global certified-reference-material-or reference-material-scaled nutrient gridded dataset GND13. Earth System Science Data 12.1, 487-499, 2020.

Becker, S., Aoyama, M., Woodward, E.M.S., Bakker, K., Coverly. S., Mahaffey, C., and Tanhua, T.: GO-SHIP Repeat Hydrography Nutrient Manual: The precise and accurate determination of dissolved inorganic nutrients in seawater, using Continuous Flow Analysis methods, In: The GO-SHIP Repeat Hydrography Manual: A Collection of Expert Reports and Guidelines, 56 , 2019, http://dx.doi.org/10.25607/OBP-555

Belgacem, M., Chiggiato, J., Borghini, M., Pavoni, B., Cerrati, G., Acri, F; Cozzi, S., Ribotti, A., Álvarez, M., Lauvset, S. K., Schroeder, K.: Quality controlled dataset of dissolved inorganic nutrients in the western Mediterranean Sea (2004-2017) from R/V oceanographic cruises. PANGAEA, https://doi.pangaea.de/10.1594/PANGAEA.904172, 2019.

Bethoux, J. P.: Oxygen consumption, new production, vertical advection and environmental evolution in the Mediterranean Sea, Deep Sea Research, Part A, Oceanographic Research Papers, 36(5), 769–781, doi:10.1016/0198-0149(89)90150-7, 1989.

Bethoux, J. P., Morin, P., Madec, C. and Gentili, B.: Phosphorus and nitrogen behaviour in the Mediterranean Sea, Deep Sea Research, Part A, Oceanographic Research Paper, 39(9), 1641–1654, doi:10.1016/0198-0149(92)90053-V, 1992.

Bethoux, J. P., Gentili, B., Morin, P., Nicolas, E., Pierre, C. and Ruiz-Pino, D.: The Mediterranean Sea : a miniature ocean for climatic and environmental studies and a key for the climatic funcioning of the North Atlantic, Progress in Oceanography, 44, 131–146, 1999.

Béthoux, J. P., Morin, P., Chaumery, C., Connan, O., Gentili, B. and Ruiz-Pino, D.: Nutrients in the Mediterranean Sea, mass balance and statistical analysis of concentrations with respect to environmental change, Marine Chemestry , 63(1–2), 155–169, doi:10.1016/S0304-4203(98)00059-0, 1998.

Béthoux, J. P., Morin, P. and Ruiz-Pino, D. P.: Temporal trends in nutrient ratios: Chemical evidence of Mediterranean ecosystem changes driven by human activity, Deep Sea Research Part II Topical Studies in Oceanography, 49(11), 2007–2016, doi:10.1016/S0967-0645(02)00024-3, 2002.

Boyd, P. W.: Beyond ocean acidification, Nature Geoscience, 4(5), 273–274, doi:10.1038/ngeo1150, 2011.

Coppola, L., Raimbault, P., Mortier, L., and Testor, P.: Monitoring the environment in the northwestern Mediterranean Sea, Eos, 100, https://doi.org/10.1029/2019EO125951, 2019.

Dickson, A. G., Afghan, J. D. and Anderson, G. C.: Reference materials for oceanic CO2 analysis: A method for the certification of total alkalinity, Marine Chemistry, 80(2–3), 185–197, doi:10.1016/S0304-4203(02)00133-0, 2003.

Fichaut, M., Garcia, M. J., Giorgetti, A., Iona, A., Kuznetsov, A., Rixen, M. and Group, M.: MEDAR/MEDATLAS 2002: A Mediterranean and Black Sea database for operational oceanography, Elsevier Oceanography Series, 69, 645–648, doi:10.1016/S0422-9894(03)80107-1, 2003.

Giorgetti, A., Partescano, E., Barth, A., Buga, L., Gatti, J., Giorgi, G., Iona A., Lipizer M., Holdsworth N., Larsen M.M., Schaap D., Vinci M., Wenzer M. :EMODnet Chemistry Spatial Data Infrastructure for marine observations and related information. Ocean & Coastal Management, 166, 9-17, 2018.

Giorgi, F.: Climate change hot-spots, Geophysical Research Letters, 33(8), 1–4, doi:10.1029/2006GL025734, 2006.

Gouretski, V. V. and Jancke, K.: Systematic errors as the cause for an apparent deep water property variability: Global analysis of the WOCE and historical hydrographic data, Progress in Oceanography, 48(4), 337–402, doi:10.1016/S0079-6611(00)00049-5, 2000.

Grasshoff, K., Kremling K., Ehrhardt M.: Methods of seawater analysis (3rd ed.), Weinheim Press, WILEY-VCH, 203-273, 1999.

Hansen, H. P. and Koroleff, F.: Determination of nutrients, Methods of Seawater Analysis, 159–228, 1999.

Hoppema, M., Velo, A., van Heuven, S., Tanhua, T., Key, R. M., Lin, X., Bakker, D. C. E., Perez, F. F., Ríos, A. F., Lo Monaco, C., Sabine, C. L., Álvarez, M. and Bellerby, R. G. J.: Consistency of cruise data of the CARINA database in the Atlantic sector of the Southern Ocean, Earth System Science Data, 1(1), 63–75, doi:10.5194/essd-1-63-2009, 2009.

Hydes, D. J.; Aoyama, M.; Aminot, A.; Bakker, K.; Becker,S.; Coverly, S.; Daniel, A.; Dickson, A. G.; Grosso, O.; Kerouel, R.; van Ooijen, J.; Sato, K.; Tanhua, T.; Woodward, E. M. S. and Zhang, J. Z. Determination of Dissolved Nutrients (N, P, SI) in Seawater With High Precision and Inter-Comparability Using Gas-Segmented Continuous Flow Analysers. In: The GO-SHIP Repeat Hydrography Manual: A Collection of Expert Reports and Guidelines. Version 1. (eds Hood, E.M., C.L. Sabine, and B.M. Sloyan). IOCCP Report Number 14, ICPO Publication Series Number 134. 87 pp., http://dx.doi.org/10.25607/OBP-555, 2010.

Dore, J. E., Houlihan, T., Hebel, D. V., Tien, G., Tupas, L., Karl, D. M.: Freezing as a method of sample preservation for the analysis of dissolved inorganic nutrients in seawater, Marine Chemistry, 53(3-4), 173-185, 1996.

Johnson, G. C., Robbins, P. E. and Hufford, G. E.: Systematic adjustments of hydrographic sections for internal consistency, Journal of Atmospheric Oceanic Technology, 18(7), 1234–1244, doi:10.1175/1520-0426(2001)018<1234:SAOHSF>2.0.CO;2, 2001.

Key, R. M., Kozyr, A., Sabine, C. L., Lee, K., Wanninkhof, R., Bullister, J. L., Feely, R. A., Millero, F. J., Mordy, C. and Peng, T. H.: A global ocean carbon climatology: Results from Global Data Analysis Project (GLODAP), Global Biogeochem. Cycles, 18(4), 1–23, doi:10.1029/2004GB002247, 2004.

Lauvset, S. K. and Tanhua, T.: A toolbox for secondary quality control on ocean chemistry and hydrographic data, Limnology and Oceanography Methods, 13(11), 601–608, doi:10.1002/lom3.10050, 2015.

Lazzari, P., Solidoro, C., Salon, S. and Bolzon, G.: Spatial variability of phosphate and nitrate in the Mediterranean Sea : A modeling approach, Deep Sea Research Part I, 108, 39–52, doi:10.1016/j.dsr.2015.12.006, 2016.

Lejeusne, C., Chevaldonné, P., Pergent-Martini, C., Boudouresque, C. F. and Pérez, T.: Climate change effects on a miniature ocean: the highly diverse, highly impacted Mediterranean Sea, Trends in Ecology and Evolution, 25(4), 250–260, doi:10.1016/j.tree.2009.10.009, 2010.

Manca, B., Burca, M., Giorgetti, A., Coatanoan, C., Garcia, M. J., & Iona, A. : Physical and biochemical averaged vertical profiles in the Mediterranean regions: an important tool to trace the climatology of water masses and to validate incoming data from operational oceanography. Journal of Marine Systems, 48(1-4), 83-116, 2004.

Martín Míguez, B., Novellino, A., Vinci, M., Claus, S., Calewaert, J. B., Vallius, H., Schmitt, T., Pititto, P., Giorgetti, A., Askew,N., Iona, S., Schaap, D., Pinardi, N., Harpham,.Q, Kater, B.J., Populus, J.,She, J., Vasilev Palazov, A., McMeel, O., Oset, P., Lear,D., Manzella, G.M.R., Gorringe, P., Simoncelli, S.,Larkin, K., Holdsworth, N., Dimitrios_Arvanitidis C., Molina-Jack M.E., Chaves-Montero M.D.M. , Herman, P.M.J., and Hernandez F.: The European marine observation and data network (EMODnet): visions and roles of the gateway to marine data in Europe. Frontiers in Marine Science, 6, (2019).

Moon, J., Lee, K., Tanhua, T., Kress, N. and Kim, I.: Temporal nutrient dynamics in the Mediterranean Sea in response to anthropogenic inputs, , 5243–5251, doi:10.1002/2016GL068788.Received, 2016.

Muniz, K., Cruzado, A., Ruiz De Villa, C. and Villa, C. R. De: Statistical analysis of nutrient data quality (nitrate and phosphate), applied to useful predictor models in the northwestern Mediterranean Sea, Methodology, 17, 221–231, 2001.

Olsen, A., Key, R. M., Heuven, S. Van, Lauvset, S. K., Velo, A., Lin, X., Schirnick, C., Kozyr, A., Tanhua, T., Hoppema, M. and Jutterström, S.: The Global Ocean Data Analysis Project version 2 (GLODAPv2) – an internally consistent data product for the world ocean, , 297–323, doi:10.5194/essd-8-297-2016, 2016.

Olsen, A., Lange, N., Key,R., Tanhua, T., Alvarez, M. et al.: GLODAPv2.2019 -an update of GLODAPv2. Earth Syst. Sci. Data, 2019, 11 (3), pp.1437 - 1461. ff10.5194/essd-11-1437-2019ff. ffhal-02315662

Pasqueron, O., Fommervault, D., Migon, C., Ortenzio, F. D., Ribera, M. and Coppola, L.: Deep-Sea Research I Temporal variability of nutrient concentrations in the northwestern Mediterranean sea (DYFAMED time-series station), Deep. Res. Part I, 100, 1–12, doi:10.1016/j.dsr.2015.02.006, 2015.

Powley, H. R., Krom, M. D. and Van Cappellen, P.: Phosphorus and nitrogen trajectories in the Mediterranean Sea (1950–2030): Diagnosing basin-wide anthropogenic nutrient enrichment, Progress in Oceanography, 162, 257–270, doi:10.1016/j.pocean.2018.03.003, 2018.

Pujo-Pay, M., Conan, P., Oriol, L., Cornet-Barthaux, V., Falco, C., Ghiglione, J. F., Goyet, C., Moutin, T. and Prieur, L.: Integrated survey of elemental stoichiometry (C, N, P) from the western to eastern Mediterranean Sea, Biogeosciences, 8(4), 883–899, doi:10.5194/bg-8-883-2011, 2011.

Sabine, C. L., Hoppema, M., Key, R. M., Tilbrook, B., Van Heuven, S., Lo Monaco, C., Metzl, N., Ishii, M., Murata, A. and Musielewicz, S.: Assessing the internal consistency of the CARINA data base in the Pacific sector of the Southern Ocean, Earth System Science Data Discussions, 2(2), 195–204, doi:10.5194/essd-2-195-2010, 2010.

Schroeder, K., Tanhua, T., Bryden, H., Alvarez, M., Chiggiato, J. and Aracri, S.: Mediterranean Sea Ship-based Hydrographic Investigations Program (Med-SHIP), Oceanography, 28(3), 12–15, doi:10.5670/oceanog.2015.71, 2015.

Schroeder, K., Chiggiato, J., Bryden, H. L., Borghini, M. and Ben Ismail, S.: Abrupt climate shift in the Western Mediterranean Sea, Scientific Reports, 1–7, doi:10.1038/srep23009, 2016.

Segura-Noguera, M., Cruzado, A. and Blasco, D.: The biogeochemistry of nutrients, dissolved oxygen and chlorophyll a in the Catalan Sea (NW Mediterranean Sea), Sci. Mar., 80(S1), 39–56, doi:10.3989/scimar.04309.20a, 2016.

Segura-Noguera, M., Cruzado, A., & Blasco, D.: Nutrient preservation, analysis precision and quality control of an oceanographic database of inorganic nutrients, dissolved oxygen and chlorophyll a from the NW Mediterranean Sea. Scientia Marina, 75(2), 321-339, 2011.

Suzuki, T., Ishii, M., Aoyama, A., Christian, J. R., Enyo, K., Kawano, T., Key, R. M., Kosugi, N., Kozyr, A., Miller, L. A., Murata, A., Nakano, T., Ono, T., Saino, T., Sasaki, K., Sasano, D., Takatani, Y., Wakita, M., and Sabine, C. L.: PACIFICA Data Synthesis Project, ORNL/CDIAC-159, NDP-092, Carbon Dioxide Information Analysis Center, Oak Ridge National Laboratory, U. S. Department of Energy, Oak Ridge, Tennessee, 2013.

Tanhua, T Hydrochemistry of water samples during MedSHIP cruise Talpro. PANGAEA, https://doi.org/10.1594/PANGAEA.902293, 2019.

Tanhua, T.: Matlab Toolbox to Perform Secondary Quality Control (2nd QC) on Hydrographic Data, ORNL CDIAC-158. Carbon Dioxide Inf. Anal. Center, Oak Ridge Natl. Lab. U.S. Dep. Energy, Oak Ridge, Tennessee, 158, doi:10.3334/CDIAC/otg.CDIAC_158, 2010a.

Tanhua, T., Brown, P. J. and Key, R. M.: CARINA : nutrient data in the Atlantic Ocean, Earth Science Data, 1, 7–24, doi:10.3334/CDIAC/otg.CARINA.ATL.V1.0, 2009.

Tanhua, T., Heuven, S. van, Key, R. M., Velo, A., Olsen, A. and Schirnick, C.: Quality control procedures and methods of the CARINA database, Earth System Scence Data, 2, 35–49, 2010b.

Tanhua, T., Hainbucher, D., Schroeder, K., Cardin, V., Álvarez, M. and Civitarese, G.: The Mediterranean Sea system: A review and an introduction to the special issue, Ocean Science, 9(5), 789–803, doi:10.5194/os-9-789-2013, 2013.

Testor, P., Bosse, A., Houpert, L., Margirier, F., Mortier, L., Legoff, H., Dausse, D., Labaste, M., Karstensen, J., Hayes, D., Olita, A., Ribotti, A., Schroeder, K., Chiggiato, J., Onken, R., Heslop, E., Mourre, B., D'ortenzio, F., Mayot, N., Lavigne, H., de Fommervault, O., Coppola, L., Prieur, L., Taillandier, V., Durrieu de Madron, X., Bourrin, F., Many, G., Damien, P., Estournel, C., Marsaleix, P., Taupier-Letage, I., Raimbault, P., Waldman, R., Bouin, M. N., Giordani, H., Caniaux, G., Somot, S., Ducrocq, V. and Conan, P.: Multiscale Observations of Deep Convection in the Northwestern Mediterranean Sea During Winter 2012–2013 Using Multiple Platforms, Journal of Geophysical Research: Oceans, 123(3), 1745–1776, doi:10.1002/2016JC012671, 2018.

Tintoré, J., Pinardi, N., Alvarez Fanjul, E., Balbin, R., Bozzano, R., Ferrarin, C.,... & Clementi, E.: Challenges for Sustained Observing and Forecasting Systems in the Mediterranean Sea. Frontiers in Marine Science, 6, 568 (2019).

Figure Captions

Figure 1. Map of the Western Mediterranean Sea showing the biogeochemical stations (in blue) and the five reference cruise stations (in red).

Figure 2. Overview of the reference cruise spatial coverage and vertical distributions of the inorganic nutrients. Top left: geographical distribution map, top right: vertical profiles of nitrate in μmol kg^{-1}, bottom left: vertical profiles of phosphate in μmol kg^{-1}, bottom right: vertical profiles of silicate in μmol kg^{-1}.

Figure 3. Scatter plots of (A.) phosphate vs nitrate (in μmol kg^{-1}) and (B.) silicate vs. nitrate (in μmol kg^{-1}). Data that have been flagged as "questionable" (flag=3) are in red, the colour bar indicates the pressure (in dbar). The black lines represent the best linear fit between the two parameters, and the corresponding equations and r^2 values are shown on each plot. Average resulting N:P ratio is 20.87, average resulting N:Si ratio is 1.05 (whole depth).

Figure 4. An example of the calculated offset for silicate between cruise 48UR20131015 and cruise 29AJ2016818 (reference cruise). Above: location of the stations being part of the crossover and statistics. Bottom left: vertical profiles of silicate data in (μmol kg^{-1}) of the two cruises that fall within the minimum distance criteria (the crossing region), below 1000 dbar. Bottom right: vertical plot of the difference between both cruises (dotted black line) with standard deviations (dashed black lines) and the weighted average of the offset (solid red line) with the weighted standard deviations (dotted red line).

Figure 5. Results of the crossover analysis for nitrate, before (grey) and after adjustment (blue). Error bars indicate the standard deviation of the absolute weighted offset. The dashed lines indicate the accuracy limit 2% for an adjustment to be recommended.

Figure 6. The same as Fig. 5 but for phosphate.

Figure 7. The same as Fig. 5 but for silicate.

Figure 8. Dataset comparison before (black) and after (blue) adjustment, showing vertical profiles of (A.) nitrate (in μmol kg^{-1}), (B.) phosphate (in μmol kg^{-1}) and (C.) silicate (in μmol kg^{-1}). Scatter plots of the adjusted data from all depths after 1st and 2nd quality control for (D.) phosphate vs nitrate (in μmol kg^{-1}) and (E.) silicate vs. nitrate (in μmol kg^{-1}). The black lines represent the best linear fit between the two parameters, and the corresponding equations and r^2 values are shown on each plot. Average resulting N:P ratio is 22.09, average resulting N:Si ratio is 0.94 (whole depth).

Figure 9. Vertical profiles of the inorganic nutrients in the dataset after adjustments and spatial coverage of each cruise (reference to cruise ID is above each map). The whole WMED adjusted product is shown in black while the data of each individual cruise are shown in blue (flag=2) and green (flag=3).

Figure 10. RMSE regional averages of water mass properties computed between the new adjusted product and MEDAR/Medatlas climatology for nitrate (A.), phosphate (B.) and silicate (C.).

Table captions

Table 1. Cruise summary table and parameters listed with number of stations and samples. Cruises were identified with an ID number and expedition code ('EXPOCODE' of format AABBYYYYMMDD with AA: country code, BB: ship code, YYYY: year, MM: month, DD: day indicative of cruise starting day)

Table 2. Cruise summary table of the reference cruises collection used in the secondary quality control, collected from 2001 to 2016.

Table 3. WOCE flags used in the original data product and in the adjusted product.

Table 4. Average and Standard deviations of nitrate, phosphate and silicate measurements by cruise and for each region with number of samples deeper than 1000db included in the 2nd QC. Average storage time: the minimum storage time defined as time difference between the cruise ending day and the 1st day of the laboratory analysis

Table 5. Summary of the suggested adjustment for nitrate, phosphate and silicate resulting from the crossover analysis. Adjustments for inorganic nutrient are multiplicative. NA: denotes not adjusted, i.e. data of cruises that could not be used in the crossover analysis, because of the lack of stations or data are outside the spatial coverage of reference cruises.

Table 6. Secondary QC toolbox results: improvements of the weighted mean of absolute offset per cruise of unadjusted and adjusted data; (n) is the number of crossovers per cruise. The numbers in red (less than 1) indicate that the cruise data are lower than the reference cruises. NA: not adjusted.

Table 7. Water mass properties and regional average concentrations of inorganic nutrients: comparison between the new adjusted product and the MEDAR/Medatlas climatology (with standard deviations and number of observations in brackets).

Figure 1

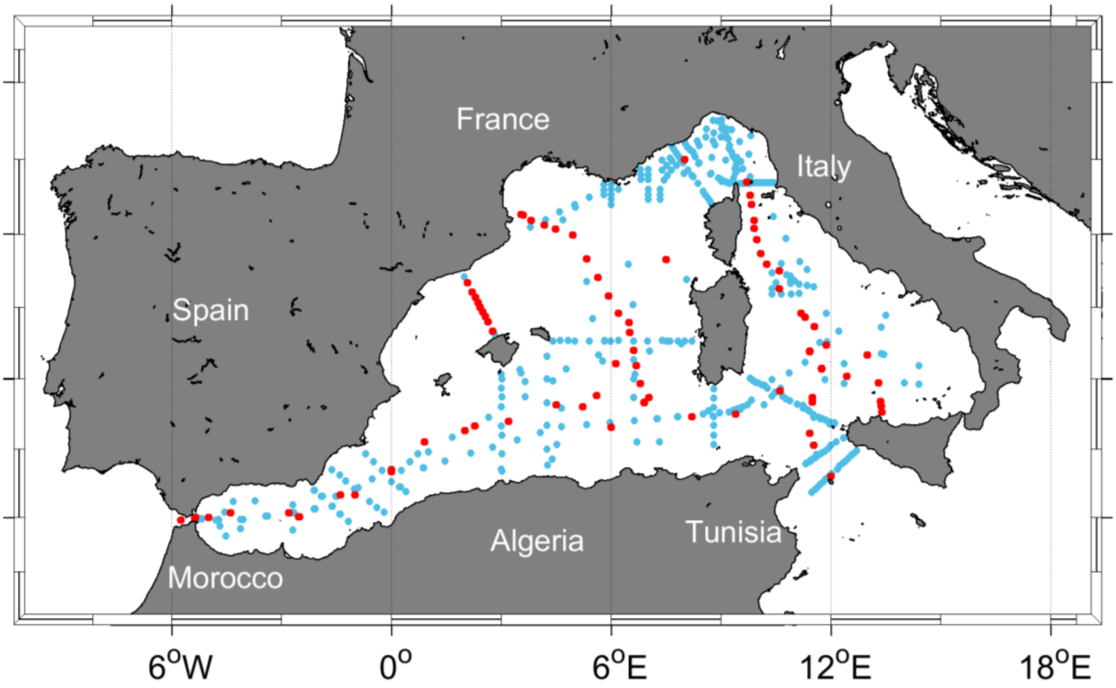

45°N
42°N
39°N
36°N
France
Italy
Spain
Morocco
Algeria
Tunisia
6°W
0°
6°E
12°E
18°E

Figure 2

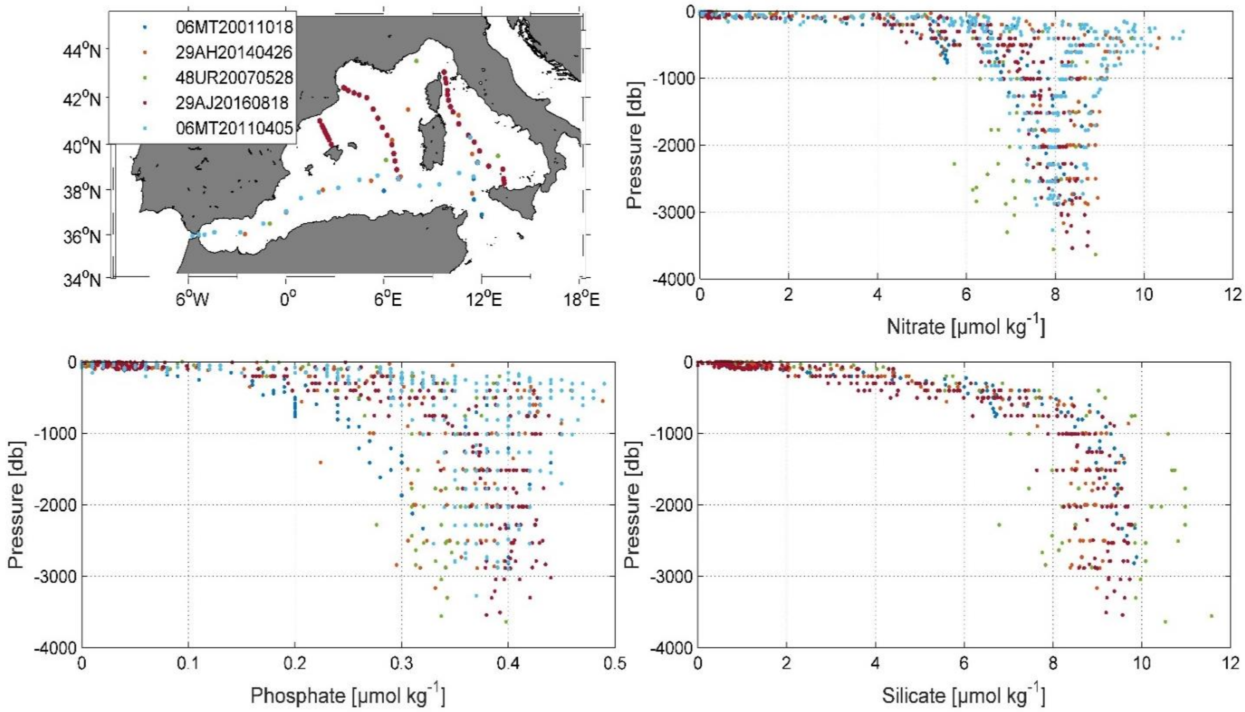

06MT20011018
29AH20140426
48UR20070528
29AJ20160818
06MT20110405
44°N
42°N
40°N
38°N
36°N
34°N
6°W
0°
6°E
12°E
18°E
Pressure [db]
Nitrate [μmol kg⁻¹]
Phosphate [μmol kg⁻¹]
Silicate [μmol kg⁻¹]

Figure 3

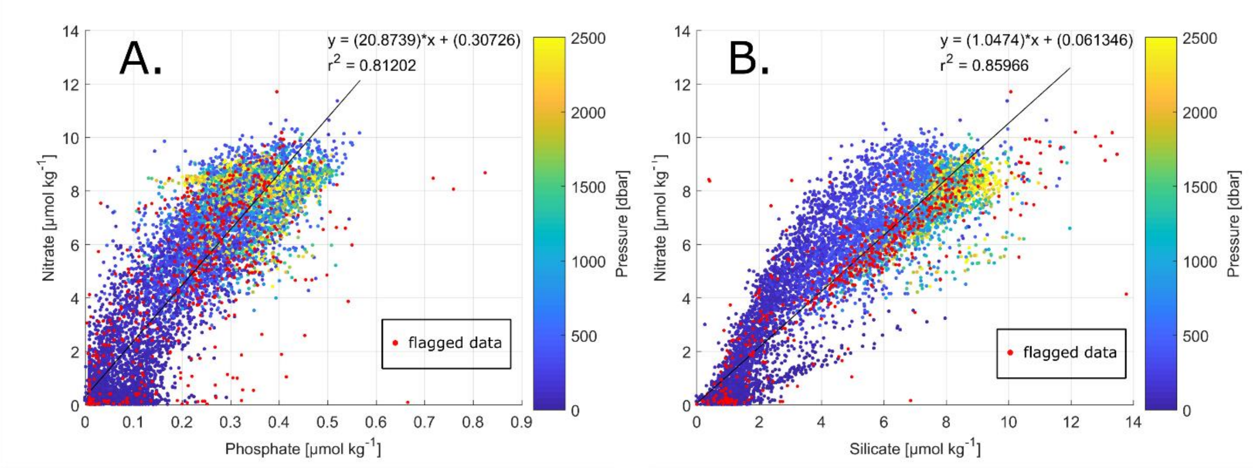

Figure 4

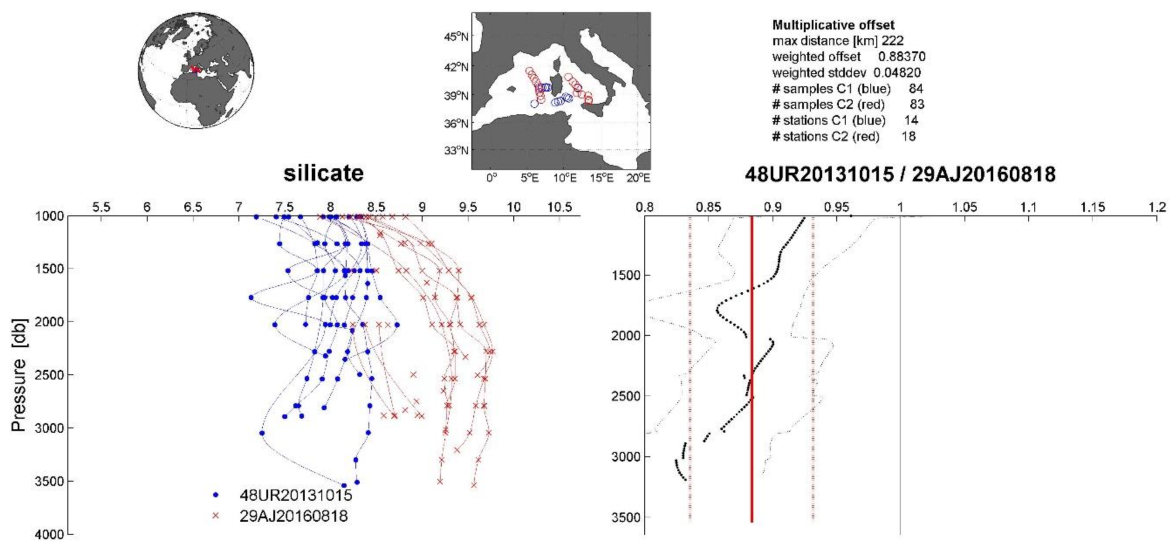

Figure 5

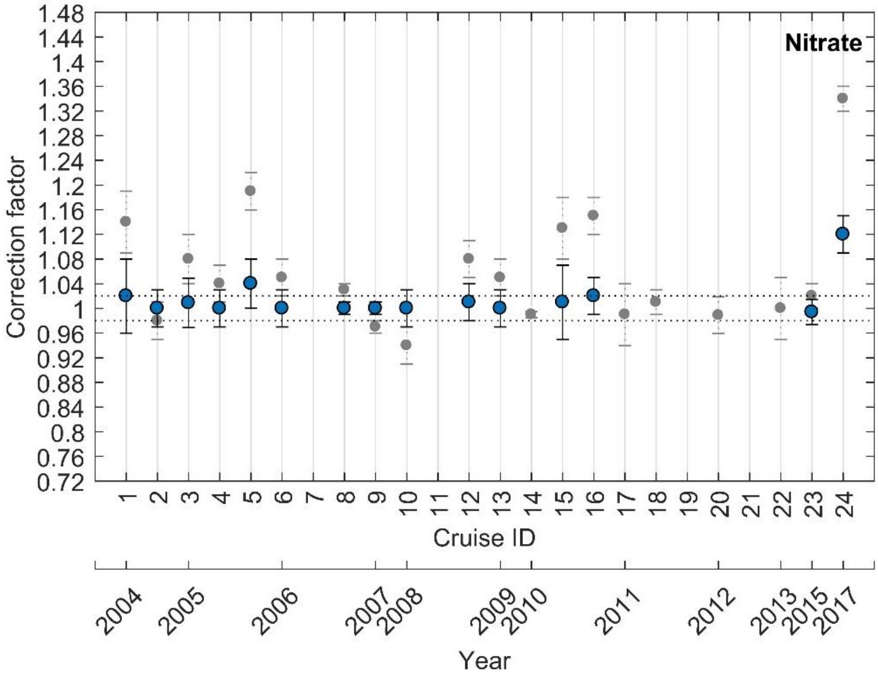

Figure 6

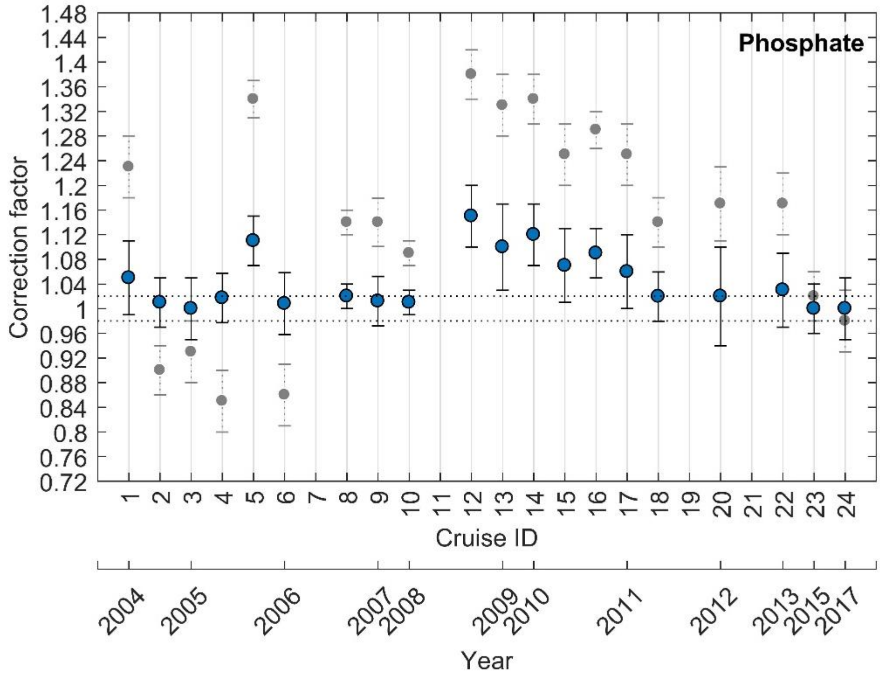
Phosphate
Correction factor
1.48
1.44
1.4
1.36
1.32
1.28
1.24
1.2
1.16
1.12
1.08
1.04
1
0.96
0.92
0.88
0.84
0.8
0.76
0.72
1 2 3 4 5 6 7 8 9 10 11 12 13 14 15 16 17 18 19 20 21 22 23 24
Cruise ID
2004 2005 2006 2007 2008 2009 2010 2011 2012 2013 2015 2017
Year

Figure 7

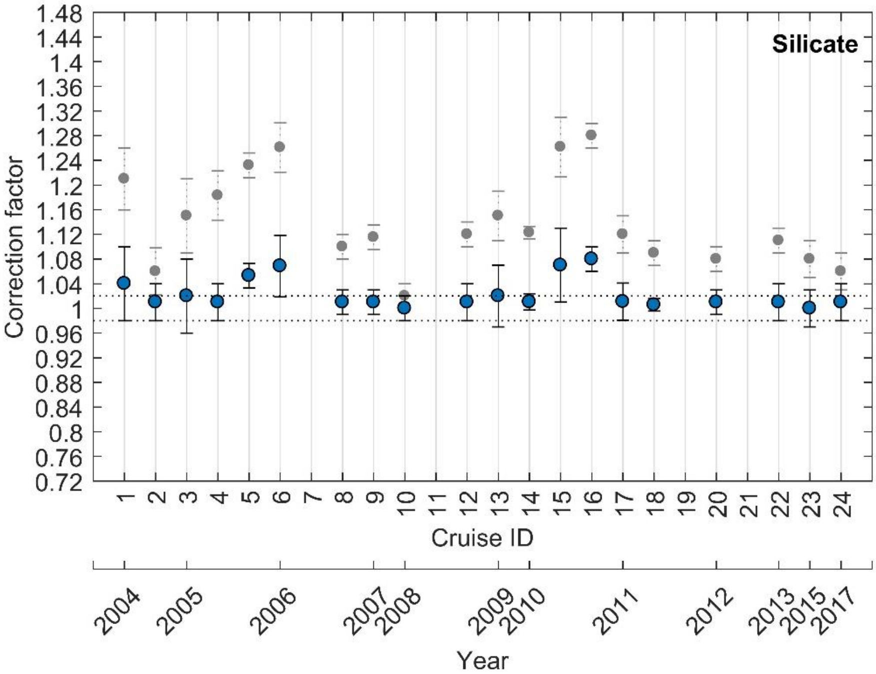
Silicate
Correction factor
1.48
1.44
1.4
1.36
1.32
1.28
1.24
1.2
1.16
1.12
1.08
1.04
1
0.96
0.92
0.88
0.84
0.8
0.76
0.72
1 2 3 4 5 6 7 8 9 10 11 12 13 14 15 16 17 18 19 20 21 22 23 24
Cruise ID
2004 2005 2006 2007 2008 2009 2010 2011 2012 2013 2015 2017
Year

Figure 8

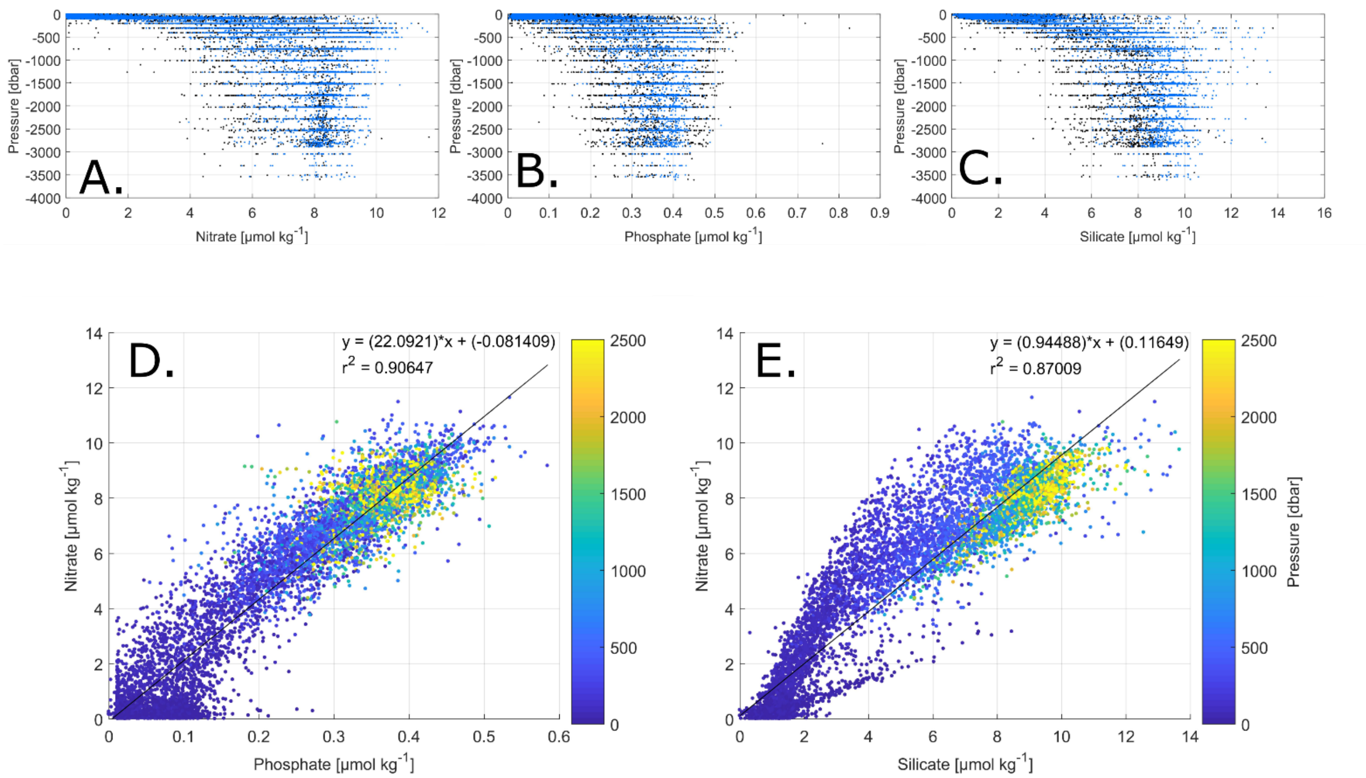

A.
B.
C.
D.
E.
Pressure [dbar]
Nitrate [µmol kg-1]
Phosphate [µmol kg-1]
Silicate [µmol kg-1]
y = (22.0921)*x + (-0.081409)
r2 = 0.90647
y = (0.94488)*x + (0.11649)
r2 = 0.87009

Figure 9

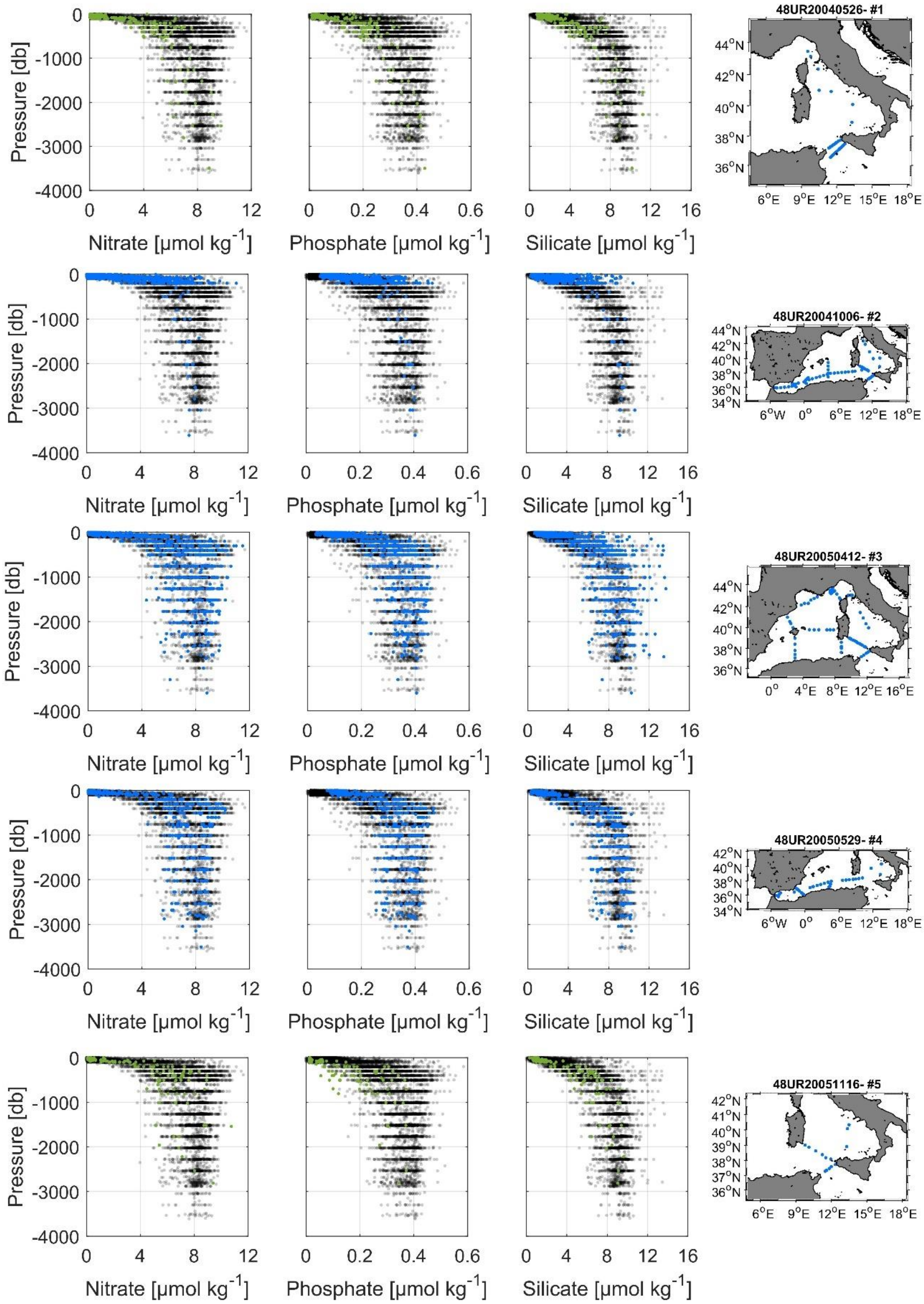

48UR20040526- #1
48UR20041006- #2
48UR20050412- #3
48UR20050529- #4
48UR20051116- #5
Pressure [db]
Nitrate [µmol kg^{-1}]
Phosphate [µmol kg^{-1}]
Silicate [µmol kg^{-1}]

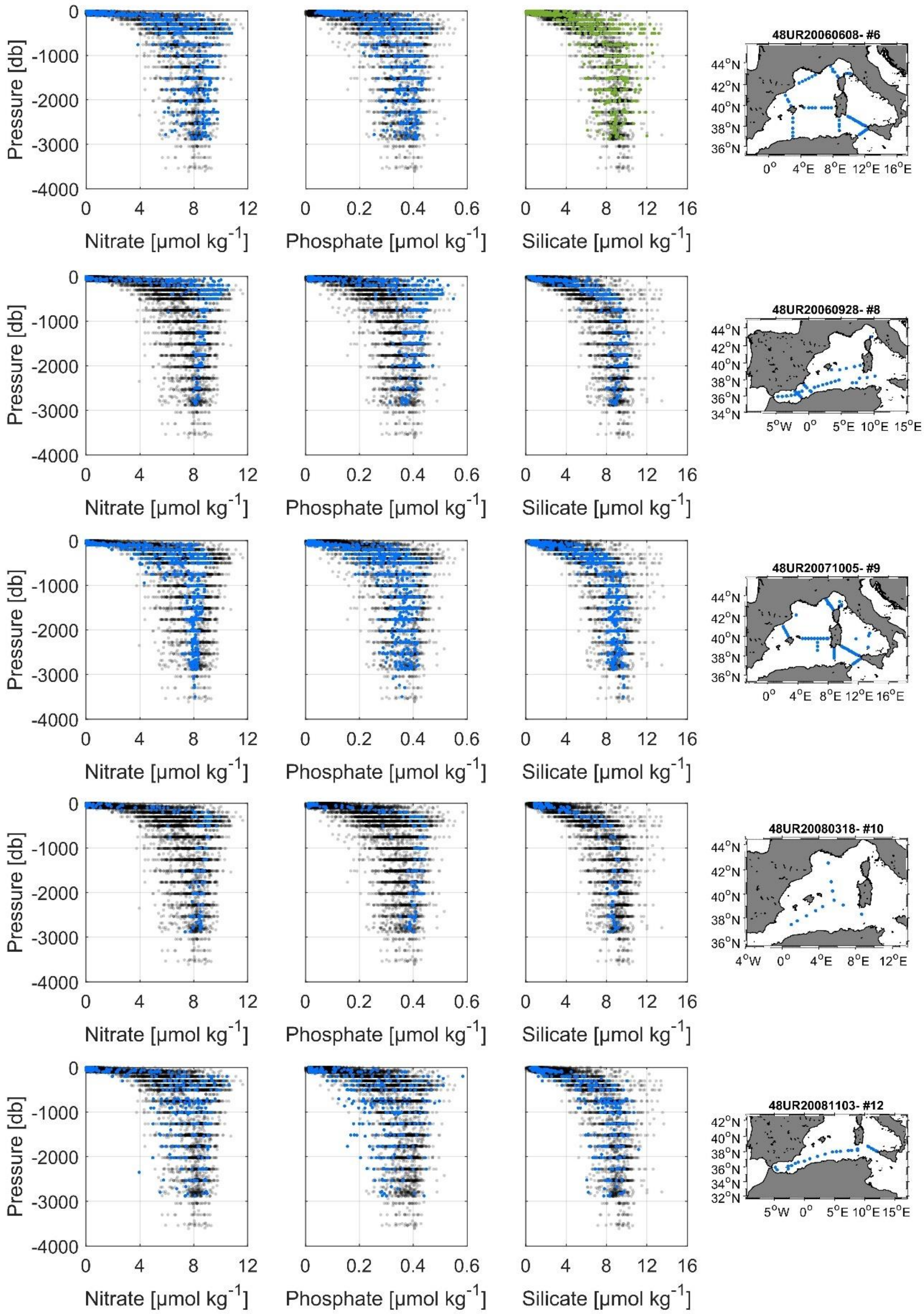

Pressure [db]
Nitrate [μmol kg^{-1}]
Phosphate [μmol kg^{-1}]
Silicate [μmol kg^{-1}]
48UR20060608- #6
48UR20060928- #8
48UR20071005- #9
48UR20080318- #10
48UR20081103- #12

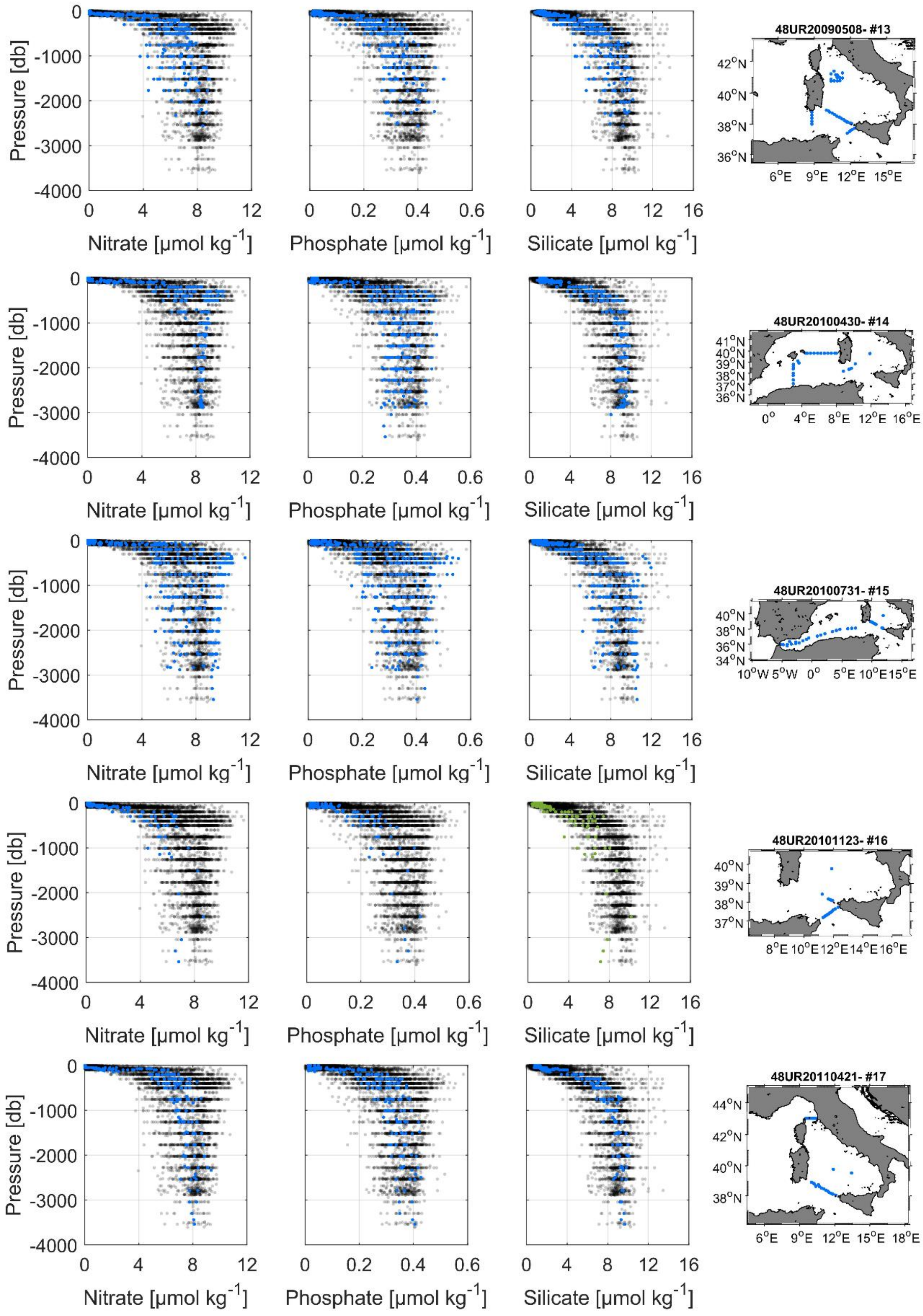
Pressure [db]
Nitrate [μmol kg^-1]
Phosphate [μmol kg^-1]
Silicate [μmol kg^-1]
48UR20090508- #13
48UR20100430- #14
48UR20100731- #15
48UR20101123- #16
48UR20110421- #17

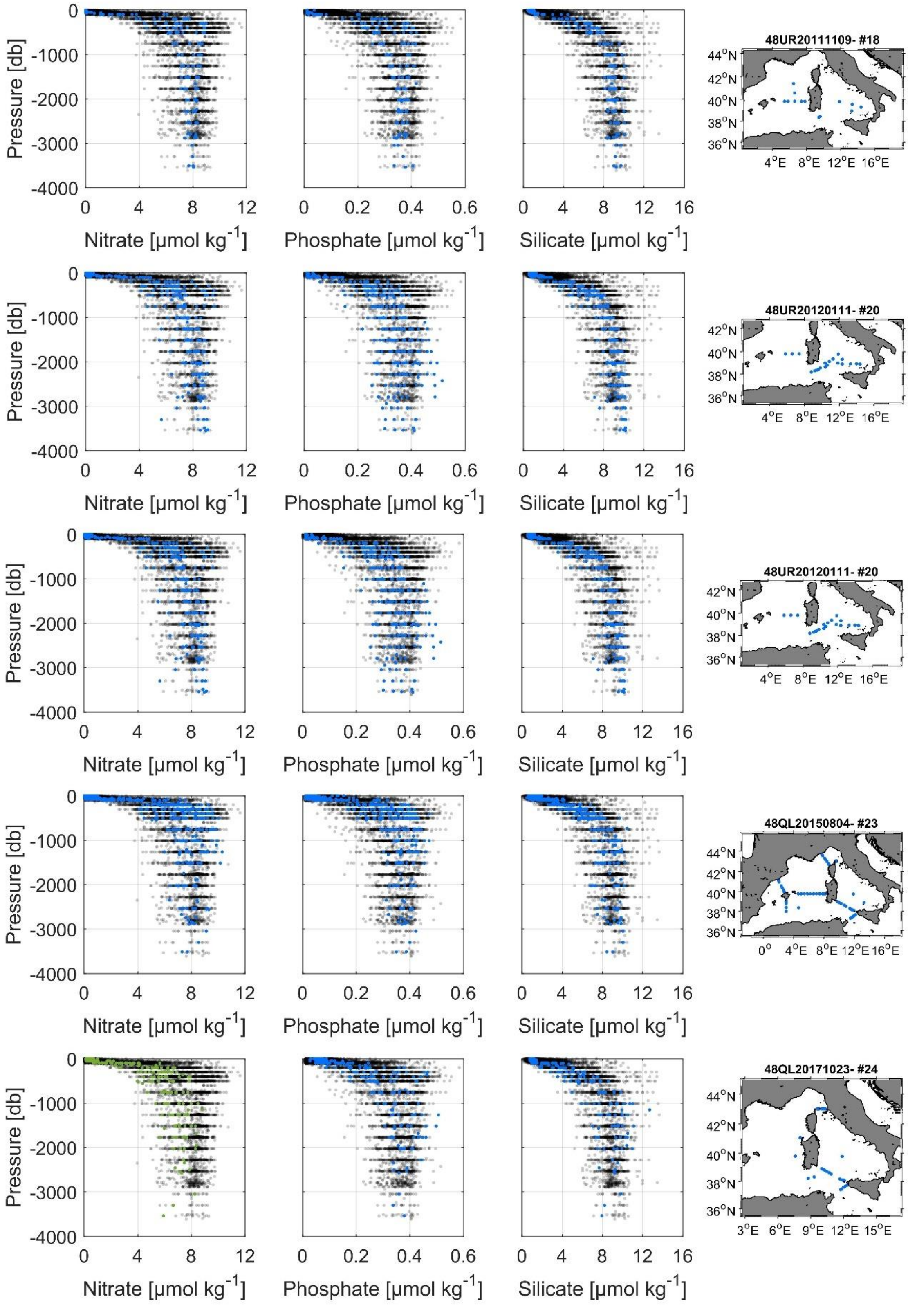
48UR20111109- #18
48UR20120111- #20
48UR20120111- #20
48QL20150804- #23
48QL20171023- #24
Pressure [db]
Nitrate [µmol kg-1]
Phosphate [µmol kg-1]
Silicate [µmol kg-1]

Figure 10

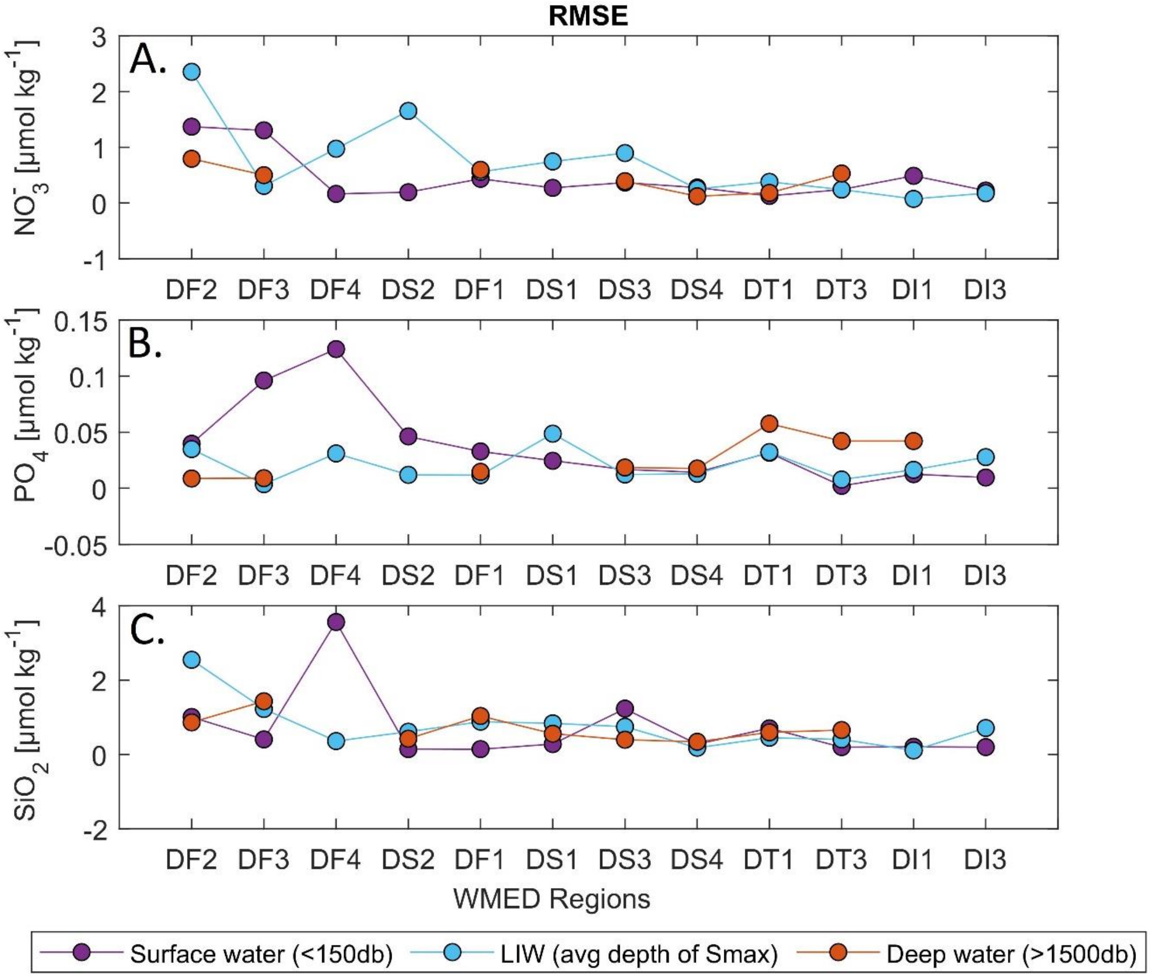
RMSE
A.
B.
C.
NO_3^- [µmol kg^{-1}]
PO_4 [µmol kg^{-1}]
SiO_2 [µmol kg^{-1}]
DF2 DF3 DF4 DS2 DF1 DS1 DS3 DS4 DT1 DT3 DI1 DI3
WMED Regions
Surface water (<150db)
LIW (avg depth of Smax)
Deep water (>1500db)

Table 1

Cruise ID (#)	Common Name	EXPOCODE	Research vessel (RV)	Date Start/End	Stations	Samples NO_3	Samples PO_4	Samples SiO_2	Maximum bottom depth (m)	Chief scientist
1	TRENDS2004/MEDGOOS8leg2	48UR20040526	Urania	26 MAY - 14 JUN 2004	36	255	253	255	3499	M. Borghini
2	MEDGOOS9	48UR20041006	Urania	6 - 25 OCT 2004	68	627	626	627	3610	M. Borghini
3	MEDOCC05/MFSTEP2	48UR20050412	Urania	12 APR - 16 MAY 2005	68	828	828	828	3598	M. Borghini
4	MEDGOOS10	48UR20050529	Urania	29 MAY - 10 JUN 2005	36	577	577	577	3505	A. Perilli
5	MEDGOOS11	48UR20051116	Urania	16 NOV - 3 DEC 2005	14	143	143	143	2810	A. Perilli, M. Borghini, M. Dibitetto
6	MEDOCC06	48UR20060608	Urania	8 JUN - 3 JUL 2006	66	787	785	787	2881	M. Borghini
7	SIRENA06	06A420060720	NRV Alliance	20 JUL - 6 AUG 2006	35	208	208	209	1854	J. Haun
8	MEDGOOS13/MEDBIO06	48UR20060928	Urania	28 SEP - 8 NOV 2006	37	519	520	520	2862	A. Ribotti
9	MEDOCC07	48UR20071005	Urania	5 - 29 OCT 2007	71	977	977	979	3497	A. Perilli
10	SESAMEIt4	48UR20080318	Urania	18 MAR - 7 APR 2008	11	164	164	164	2882	C. Santinelli
11	SESAMEIT5	48UR20080905	Urania	5 - 16 SEP 2008	12	74	74	74	536	S. Sparnocchia, G.P. Gasparini, M. Borghini
12	MEDCO08	48UR20081103	Urania	3 - 24 NOV 2008	24	342	350	348	2880	A. Ribotti
13	TYRRMOUNTS	48UR20090508	Urania	8 MAY - 3 JUN 2009	41	430	441	440	2559	G.P. Gasparini
14	BIOFUN010	48UR20100430	Urania	30 APR - 17 MAY 2010	26	405	405	405	3540	E. Manini, S. Aliani
15	VENUS1	48UR20100731	Urania	31 JUL - 25 AUG 2010	32	431	432	428	3544	G.P. Gasparini, M. Borghini
16	BONSIC2010	48UR20101123	Urania	23 NOV - 9 DEC 2010	18	144	143	143	3540	A. Ribotti
17	EUROFLEET11	48UR20110421	Urania	21 APR - 8 MAY 2011	28	277	275	277	3540	G.P. Gasparini, M. Borghini
18	BONIFACIO2011	48UR20111109	Urania	9 - 23 NOV 2011	13	180	180	181	3541	A. Ribotti, G. La Spada, M. Borghini
19	TOSCA2011	48MG20111210	Maria Grazia	10 - 20 DEC 2011	21	310	310	309	2728	M. Borghini
20	ICHNUSSA12	48UR20120111	Urania	11 - 27 JAN 2012	21	353	352	323	3551	A. Ribotti
21	EUROFLEET2012	48UR20121108	Urania	8 - 26 NOV 2012	53	429	434	434	2633	M. Borghini
22	ICHNUSSA13	48UR20131015	Urania	15 - 29 OCT 2013	37	405	404	405	3540	A. Ribotti
23	OCEANCERTAIN15	48QL20150804	Minerva Uno	4 - 29 AUG 2015	71	531	531	531	3513	J. Chiggiato
24	ICHNUSSA17/INFRAOCE17	48QL20171023	Minerva Uno	23 OCT- 28 NOV 2017	31	251	254	254	3536	A. Ribotti, S. Sparnocchia, M. Borghini

Table 2

Common name	EXPOCODE	Date Start/End	Stations	NO3 Sample	PO4 Sample	SiO2 Sample	Source	Nutrient PI	Chief scientist
M51/2	06MT20011018	18 OCT - 11 NOV 2001	6	79	79	82	GLODAPv2	B. Schneider	W. Roether
TRANSMED_LEGII	48UR20070528	28 MAY- 12 JUN 2007	4	78	77	78	CARIMED (not yet available)	S. Cozzi, V. Ibello	M. Azzaro
M84/3	06MT20110405	5 - 28 APR 2011	20	339	343	-	GLODAPv2	G. Civitarese	T. Tanhua
HOTMIX	29AH20140426	26 APR- 31 MAY 2014	18	144	140	144	CARIMED (not yet available)	XA Álvarez-Salgado	J. Aristegui
TALPro-2016	29AJ20160818	18 - 28 AUG 2016	42	293	293	293	MedSHIP programme	L. Coppola	L. Jullion, K. Schroeder

Table 3

WOCE flag value	Interpretation in original dataset	Interpretation in adjusted product
2	Acceptable/ measured	Adjusted and acceptable
3	Questionable/not used	Adjusted and recommended questionable
9	not measured/no data	-

Table 4

Cruise ID	EXPOCODE/ Region	Regional Avg NO_3	std NO_3	Regional Avg PO_4	std PO_4	Regional Avg SiO_2	std SiO_2	# samples	Avg storage (in days)
1	48UR20040526/		**1.25**		**0.062**		**1.64**	21	131
	DT1-Tyrrhenian North	6.07	1.32	0.26	0.065	6.92	1.83	16	
	DT3-Tyrrhenian South	7.03	0.51	0.31	0.02	7.66	0.53	5	
2	48UR20041006/		**0.59**		**0.029**		**0.81**	21	251
	DT1-Tyrrhenian North	7.68	0.53	0.41	0.031	8.74	0.75	15	
	DT3-Tyrrhenian South	8.17	0.60	0.41	0.025	9.31	0.87	6	
3	48UR20050412/		**1.15**		**0.050**		**1.41**	233	135
	DF2-Gulf of Lion	7.89	0.98	0.40	0.044	8.17	1.065	24	
	DF3-Liguro-Provençal	7.45	1.08	0.41	0.05	7.72	1.10	66	
	DS2-Balearic Sea	7.44	1.14	0.40	0.039	7.68	1.47	21	
	DF1-Algero-Provençal	7.87	1.16	0.41	0.043	8.88	1.96	42	
	DS3-Algerian West	7.7	0.816	0.39	0.048	8.14	0.941	23	
	DT1-Tyrrhenian North	6.57	1.065	0.36	0.047	7.41	1.15	21	
	DT3-Tyrrhenian South	6.52	1.12	0.36	0.05	7.56	1.42	22	
	DI1-Sardinia Channel	7.22	1.065	0.40	0.04	8.08	1.11	14	
4	48UR20050529/		**1.13**		**0.057**		**1.08**	205	314
	DS1-Alboran Sea	6.4	1.15	0.38	0.041	6.26	1.02	32	
	DS3-Algerian West	7.6	1.13	0.41	0.06	7.33	0.99	73	
	DS4-Algerian East	7.48	1.13	0.41	0.06	7.50	1.23	47	
	DT1-Tyrrhenian North	7.24	0.44	0.42	0.03	7.91	0.56	16	
	DT3-Tyrrhenian South	7.70	0.38	0.41	0.03	7.55	0.36	14	
	DI1-Sardinia Channel	7.58	1.08	0.43	0.049	7.42	0.82	23	
5	48UR20051116/		**1.35**		**0.078**		**0.98**	16	738
	DT1-Tyrrhenian North	5.68	1.26	0.19	0.08	6.30	0.92	10	
	DT3-Tyrrhenian South	6.71	1.51	0.20	0.06	6.86	1.065	5	
	DI1-Sardinia Channel	6.29	0	0.26	0	7.53	0	1	
6	48UR20060608/		**1.16**		**0.054**		**1.47**	221	27
	DF2-Gulf of Lion	7.69	1.02	0.42	0.04	7.089	1.04	27	
	DF3-Liguro-Provençal	8.08	0.78	0.43	0.04	7.41	1.21	35	
	DS2-Balearic Sea	8.06	0.9	0.43	0.03	7.07	1.18	30	
	DF1-Algero-Provençal	7.97	1.16	0.44	0.05	7.34	1.32	61	
	DS3-Algerian West	8.39	0.9	0.42	0.03	8.5	2	28	
	DT3-Tyrrhenian South	6.39	1.28	0.36	0.06	6.86	1.7	26	
	DI1-Sardinia Channel	8.04	0.85	0.43	0.04	7.77	1.25	14	
7	06A420060720		-		-		-	-	1367
8	48UR20060928/		**0.71**		**0.036**		**0.76**	179	606
	DS2-Balearic Sea	7.97	0.17	0.33	0.017	7.84	0.27	4	
	DF1-Algero-Provençal	8.17	0.22	0.33	0.026	8.11	0.3	22	
	DS1-Alboran Sea	8.2	0.14	0.35	0.02	8.59	0.35	47	
	DS3-Algerian West	7.93	0.89	0.33	0.03	8.09	0.91	70	
	DS4-Algerian East	7.98	0.68	0.34	0.04	8.01	0.7	28	
	DT3-Tyrrhenian South	6.2	1.51	0.28	0.04	6.71	1.45	3	
	DI1-Sardinia Channel	7.66	0.6	0.28	0.02	8.00	0.49	5	
9	48UR20071005/		**0.89**		**0.040**		**0.86**	302	751
	DF2-Gulf of Lion	8.41	0.08	0.31	0.01	7.43	0.02	4	
	DF3-Liguro-Provençal	8.17	1.08	0.31	0.03	7.64	1.08	81	
	DS2-Balearic Sea	8.17	0.43	0.31	0.02	7.58	0.39	29	
	DF1-Algero-Provençal	8.33	0.6	0.32	0.03	7.79	0.69	82	
	DS4-Algerian East	8.41	0.2	0.33	0.018	7.90	0.26	19	
	DT1-Tyrrhenian North	7.83	0.41	0.28	0.03	8.26	0.55	26	
	DT3-Tyrrhenian South	7.49	1.22	0.28	0.05	7.71	1.26	38	
	DI1-Sardinia Channel	7.92	1.05	0.33	0.02	8.26	0.41	23	
10	48UR20080318/		**0.51**		**0.026**		**0.34**	66	31
	DF2-Gulf of Lion	8.54	0.6	0.35	0.03	8.62	0.43	5	
	DS2-Balearic Sea	9.12	0.18	0.38	0.01	8.40	0.21	9	
	DF1-Algero-Provençal	9.02	0.36	0.38	0.03	8.65	0.25	15	
	DS3-Algerian West	8.93	0.46	0.36	0.01	8.69	0.35	20	
	DS4-Algerian East	8.43	0.25	0.38	0.02	8.32	0.22	10	
	DI1-Sardinia Channel	7.62	0.6	0.34	0.03	8.49	0.36	3	
11*	48UR20080905		-		-		-	-	211
12	48UR20081103/		**1.11**		**0.077**		**0.10**	110	536
	DS1-Alboran Sea	6.4	1.21	0.21	0.06	7.20	1.43	26	

	DS3-Algerian West	7.58	0.9	0.27	0.1	7.89	0.9	30	
	DS4-Algerian East	7.15	1.04	0.23	0.04	7.38	0.9	35	
	DT3-Tyrrhenian South	7.44	0.5	0.22	0.05	8.28	0.4	10	
	DI1-Sardinia Channel	7.40	1.23	0.17	0.04	8.09	0.45	9	
13	48UR20090508/		**1.41**		**0.051**		**1.42**	88	164
	DT1-Tyrrhenian North	5.95	1.55	0.24	0.05	6.28	1.58	46	
	DT3-Tyrrhenian South	6.76	0.77	0.24	0.03	7.37	0.77	29	
	DI1-Sardinia Channel	7.62	1.1	0.28	0.05	7.76	0.9	13	
14	48UR20100430/		**1.06**		**0.036**		**1.03**	159	213
	DS2-Balearic Sea	7.66	1.6	0.25	0.03	7.38	1.75	33	
	DF1-Algero-Provençal	8.43	0.29	0.26	0.03	8.06	0.31	61	
	DS3-Algerian West	8.5	0.14	0.26	0.03	8.25	0.3	26	
	DT1-Tyrrhenian North	6.88	0.8	0.23	0.022	7.17	0.77	11	
	DT3-Tyrrhenian South	6.38	1.35	0.22	0.01	6.76	1.56	7	
	DI1-Sardinia Channel	7.71	0.87	0.23	0.02	7.80	0.74	21	
15	48UR20100731/		**1.34**		**0.053**		**0.14**	149	213
	DS1-Alboran Sea	7.30	1.18	0.29	0.05	7.21	1.11	25	
	DS3-Algerian West	7.67	1.15	0.28	0.045	7.24	1.16	54	
	DS4-Algerian East	7.38	0.89	0.29	0.03	7.00	0.78	29	
	DT1-Tyrrhenian North	7.66	0.96	0.29	0.05	7.89	1.07	10	
	DT3-Tyrrhenian South	5.4	0.67	0.22	0.01	5.52	1.56	30	
	DI1-Sardinia Channel	4.92	0	0.20	0	5.55	0	1	
16	48UR20101123/		**1.02**		**0.045**		**1.02**	14	170
	DT1-Tyrrhenian North	6.34	0.87	0.27	0.02	6.12	0.87	8	
	DT3-Tyrrhenian South	5.43	1.02	0.22	0.04	5.08	0.9	6	
17	48UR20110421/		**0.62**		**0.029**		**0.52**	56	160
	DT1-Tyrrhenian North	7.77	0.45	0.28	0.02	8.11	0.35	21	
	DT3-Tyrrhenian South	7.76	0.7	0.28	0.03	8.017	0.6	35	
18	48UR20111109/		**0.68**		**0.025**		**0.70**	77	74
	DF3-Liguro-Provençal	6.68	0	0.33	0	6.26	0	1	
	DF1-Algero-Provençal	8.17	0.5	0.32	0.01	8.16	0.66	43	
	DT1-Tyrrhenian North	7.26	0.93	0.29	0.02	8.15	1.03	12	
	DT3-Tyrrhenian South	7.61	0.37	0.30	0.02	8.18	0.35	11	
	DI1-Sardinia Channel	7.64	0.45	0.29	0.01	8.08	0.41	10	
19*	48MG20111210		-		-		-	-	38
20	48UR20120111/		**0.97**		**0.051**		**0.26**	152	317
	DF1-Algero-Provençal	8.45	0.49	0.31	0.039	7.91	0.53	23	
	DT1-Tyrrhenian North	7.67	0.83	0.27	0.02	8.29	0.8	30	
	DT3-Tyrrhenian South	7.65	1.06	0.31	0.06	8.03	1.26	69	
	DI1-Sardinia Channel	7.65	0.96	0.31	0.03	7.86	0.78	30	
21*	48UR20121108		-		-		-	-	72
22	48UR20131015/		**1.03**		**0.043**		**0.79**	98	76
	DF1-Algero-Provençal	8.54	0.64	0.33	0.02	7.96	0.38	36	
	DS4-Algerian East	7.67	1.28	0.27	0.04	6.82	1.07	8	
	DT1-Tyrrhenian North	6.47	0.83	0.24	0.025	7.12	0.84	10	
	DT3-Tyrrhenian South	7.81	0.71	0.30	0.03	8.09	0.65	28	
	DI1-Sardinia Channel	7.32	0.99	0.27	0.02	7.47	0.89	16	
23	48QL20150804/		**0.84**		**0.038**		**0.85**	94	30
	DF3-Liguro-Provençal	8.51	0.96	0.39	0.03	8.06	0.85	23	
	DS2-Balearic Sea	7.75	0.66	0.36	0.02	7.86	0.81	20	
	DF1-Algero-Provençal	7.9	0.59	0.37	0.03	8.34	0.68	23	
	DS3-Algerian West	7.84	0.67	0.36	0.02	7.75	0.68	6	
	DT1-Tyrrhenian North	7.92	0.61	0.37	0.02	8.75	0.4	8	
	DT3-Tyrrhenian South	7.23	0.75	0.34	0.025	8.2	0.94	13	
	DI1-Sardinia Channel	6.30	0	0.25	0	5.36	0	1	
24	48QL20171023/		**0.68**		**0.055**		**1.24**	55	30
	DF3-Liguro-Provençal	6.63	0.41	0.40	0.05	10.76	1.07	3	
	DF1-Algero-Provençal	5.14	0.7	0.43	0.02	7.94	1.19	6	
	DT1-Tyrrhenian North	4.98	0.58	0.36	0.02	8.10	0.87	9	
	DT3-Tyrrhenian South	5.43	0.5	0.36	0.04	9.03	0.87	26	
	DI1-Sardinia Channel	5.16	0.76	0.41	0.07	7.58	1.17	11	

(*) cruise not included in the 2nd QC (Section 4.)

in bold: the overall standard deviation by cruise; in normal font: regional standard deviation by cruise

Table 5

Cruise ID	EXPOCODE	NO_3 (x)	PO_4 (x)	SiO_2 (x)
1	48UR20040526	1.14	1.23	1.21
2	48UR20041006	0.98	0.9	1.06
3	48UR20050412	1.08	0.93	1.15
4	48UR20050529	1.04	0.85	1.183
5	48UR20051116	1.19	1.34	1.232
6	48UR20060608	1.05	0.86	1.261
7	06A420060720*	-	-	-
8	48UR20060928	1.03	1.14	1.1
9	48UR20071005	0.97	1.14	1.115
10	48UR20080318	0.94	1.09	1.02
11	48UR20080905*	-	-	-
12	48UR20081103	1.08	1.38	1.12
13	48UR20090508	1.05	1.33	1.15
14	48UR20100430	NA	1.34	1.123
15	48UR20100731	1.13	1.25	1.262
16	48UR20101123	1.15	1.29	1.28
17	48UR20110421	NA	1.25	1.12
18	48UR20111109	NA	1.14	1.09
19	48MG20111210*	-	-	-
20	48UR20120111	NA	1.17	1.08
21	48UR20121108*	-	-	-
22	48UR20131015	NA	1.17	1.11
23	48QL20150804	1.02	1.02	1.08
24	48QL20171023	1.34	0.98	1.06

(*) cruise not included in the 2ndQC (Section 4.)

Table 6

Cruise ID	EXPOCODE	NO_3 [%]			PO_4[%]			SiO_2[%]		
		n	*unadjusted*	*adjusted*	*n*	*unadjusted*	*adjusted*	*n*	*unadjusted*	*adjusted*
1	48UR20040526	2	0.86	0.98	2	0.77	0.95	1	0.79	0.96
2	48UR20041006	2	1.02	1.00	2	1.10	0.99	1	0.94	0.99
3	48UR20050412	5	0.92	0.99	5	1.07	1.00	4	0.85	0.98
4	48UR20050529	5	0.96	1.00	5	1.15	0.98	4	0.82	0.99
5	48UR20051116	2	0.81	0.96	1	0.66	0.89	1	0.77	0.95
6	48UR20060608	5	0.95	1.00	5	1.14	0.99	4	0.74	0.93
7	06A420060720	0	-	-	0	-	-	0	-	-
8	48UR20060928	4	0.97	1.00	4	0.86	0.98	3	0.90	0.99
9	48UR20071005	5	1.03	1.00	5	0.86	0.98	4	0.88	0.99
10	48UR20080318	3	1.06	1.00	3	0.91	0.99	2	0.98	1.00
11	48UR20080905	0	-	-	0	-	-	0	-	-
12	48UR20081103	5	0.92	0.99	5	0.62	0.85	4	0.88	0.99
13	48UR20090508	3	0.95	1.00	3	0.67	0.90	2	0.85	0.98
14	48UR20100430	4	1.01	NA	4	0.66	0.88	3	0.88	0.99
15	48UR20100731	5	0.87	0.99	5	0.75	0.93	4	0.74	0.93
16	48UR20101123	1	0.85	0.98	1	0.71	0.91	1	0.72	0.92
17	48UR20110421	2	1.01	NA	2	0.75	0.94	1	0.88	0.99
18	48UR20111109	4	0.99	NA	4	0.86	0.98	3	0.91	0.99
19	48MG20111210	0	-	-	0	-	-	0	-	-
20	48UR20120111	4	1.01	NA	4	0.83	0.98	3	0.92	0.99
21	48UR20121108	0	-	-	0	-	-	0	-	-
22	48UR20131015	4	1.00	NA	4	0.83	0.97	3	0.89	0.99
23	48QL20150804	5	0.98	1.00	5	0.98	1.00	4	0.92	1.00
24	48QL20171023	3	0.66	0.88	3	1.02	1.00	2	0.94	0.99

red: data lower than reference

Table 7

Region/ Water mass	NO3 (µmol kg^{-1})		PO4 (µmol kg^{-1})		SiO2 (µmol kg^{-1})	
	Avg new Product	Avg Medar	Avg new Product	Avg Medar	Avg new Product	Avg Medar
DF2- Gulf of Lion						
surface water (0-150db)	2.68±2.53(68)**	1.7±1.1	0.15±0.06(68)	0.13±0.04	2.91±1.33(68)	1.72±0.64
LIW core (S_{max} depth range: 300-500db)	8.49±0.18(17)	6.13±0.32	0.38±0.02(17)	0.34±0.01	8.67±0.69(17)	6.12±0.61
Deep water (>1500db)	8.03±0.43(33)	7.64±0.31	0.37±0.01(33)	0.37±0.015	8.7±0.67(33)	7.95±0.06
DF3- Liguro-Provençal						
surface water (0-150db)	2.31±2.4(205)	3.0±2.6	0.12±0.07(205)	0.19±0.05	2.45±1.05(205)	2.16±1.05
LIW core (S_{max} depth range: 300-500db)	8.05±0.18(76)	7.74±0.13	0.36±0.01(76)	0.35±0.01	7.49±0.55(76)	6.26±0.60
Deep water (>1500db)	8.18±0.25(142)	7.79±0.04	0.37±0.02(142)	1.03±1.29	8.98±0.39(142)	7.60±0.21
DF4- Ligurian East						
surface water (0-150db)	0.7±0.69(228)	0.61±1.03	0.05±0.02(228)	0.18±0.02	1.37±0.45(228)	1.27±1.86
LIW core (S_{max} depth range: 300-500db)	6.8±0.4(23)	5.54±0	0.3±0.02(21)	0.36±0.06	5.86±0.9(24)	4.86±0
Deep water (>1500db)	-	-	-	-	-	-
DS2- Balearic Sea						
surface water (0-150db)	1.32±1.46(196)	1.19±1.5	0.08±0.04(196)	0.11±0.04	1.61±0.64(196)	1.54±0.78
LIW core (S_{max} depth range: 300-500db)	8.32±0.32(58)	6.92±0.12	0.37±0.02(60)	0.39±0.003	7.31±0.9(60)	7.55±0.62
Deep water (>1500db)	8.2±0.35(88)	-	0.37±0.01(88)	-	8.71±0.51(88)	8.45±0.8
DF1- Algero-Provençal						
surface water (0-150db)	0.87±0.85(372)	1.08±1.7	0.05±0.02(372)	0.07±0.05	1.42±0.3(372)	1.28±0.73
LIW core (S_{max} depth range: 300-500db)	8.07±0.34(126)	7.51±0.18	0.36±0.02(126)	0.34±0.008	6.84±0.95(126)	5.96±0.77
Deep water (>1500db)	8.36±0.27(300)	7.87±0.13	0.38±0.02(300)	0.38±0.001	9.01±0.33(300)	8.18±0.10
DS1- Alboran Sea						
surface water (0-150db)	2.75±2.87(299)	2.51±2.23	0.17±0.11(299)	0.16±0.07	2.07±1.38(299)	2.31±1.14
LIW core (S_{max} depth range: 400-600db)	8.89±0.4(77)	8.14±0.11	0.42±0.02(77)	0.37±0.008	8.77±1.66(76)	7.95±0.34
Deep water (>1500db)	7.72±0.81(65)	-	0.36±0.04(65)	-	8.98±0.63(65)	8.16±0
DS3- Algerian West						
surface water (0-150db)	1.8±1.88(254)	1.82±2.01	0.11±0.05(354)	0.11±0.06	1.71±0.68(354)	2.10±0.91
LIW core (S_{max} depth range: 400-600db)	9.33±0.08(70)	8.28±0.15	0.41±0(73)	0.38±0.012	8.1±0.53(72)	6.68±0.80
Deep water (>1500db)	8.37±0.27(246)	8.047±0.013	0.37±0.02(246)	0.36±0.006	9.22±0.35(246)	8.87±0.23
DS4- Algerian East						
surface water (0-150db)	0.94±0.77(170)	0.75±1.26	0.07±0.02(170)	0.05±0.03	1.53±0.12(170)	1.35±0.52
LIW core (S_{max} depth range: 400-600db)	8.5±0.25(43)	8.60±0.06	0.38±0.03(43)	0.38±0.008	7.27±0.67(42)	7.092±0.55
Deep water (>1500db)	7.94±0.24(132)	8.06±0.06	0.36±0.02(132)	0.38±0.006	8.73±0.38(132)	9.04±0.24
DT1- Tyrrhenian North						
surface water (0-150db)	1.03±1.14(231)	0.88±1.2	0.06±0.02(231)	0.09±0.03	1.64±0.52(231)	2.19±0.59
LIW core (S_{max} depth range: 400-600db)	5.95±0.49(43)	5.86±0.36	0.27±0.03(44)	0.308±0.02	7.06±0.08(44)	6.76±0.59
Deep water (>1500db)	7.75±0.37(194)	7.12±0.47	0.36±0.03(194)	0.40±0.02	9.19±0.47(194)	7.51±0.49
DT3- Tyrrhenian South						
surface water (0-150db)	1.21±1.38(711)	1.23±1.80	0.06±0.03(711)	0.061±0.04	1.58±0.61(711)	1.55±1.05
LIW core (S_{max} depth range: 300-500db)	6.2±0.28(225)	6.42±0.01	0.26±0.02(225)	0.254±0.005	6.28±0.65(224)	6.68±0.44
Deep water (>1500db)	7.88±0.4(227)	7.12±0.26	0.37±0.02(227)	0.31±0.007	9.04±0.52(227)	8.02±0.07
DI1- Sardinia Channel						
surface water (0-150db)	1.22±1.39(271)	1.42±1.95	0.07±0.03(271)	0.064±0.03	1.57±0.68(271)	1.39±1.01
LIW core (S_{max} depth range: 300-500db)	6.52±0.17(89)	6.45±0.22	0.27±0.02(89)	0.250±0.01	6.36±0.67(89)	6.27±0.70
Deep water (>1500db)	7.91±0.62(107)	-	0.37±0.03(107)	0.32±0	8.64±0.91(107)	-
DI3- Sicily Strait						
surface water (0-150db)	0.87±0.68(583)	0.77±0.81	0.06±0.02(583)	0.063±0.02	1.53±0.29(583)	1.44±0.58
LIW core (S_{max} depth range: 200-400db)	4.95±0.47(80)	5.14±0.14	0.21±0.02(78)	0.194±0.004	5.26±0.79(81)	6.744±0.41
Deep water (>1500db)	-	-	-	-	-	-

**Average (Avg) ± standard deviation of inorganic nutrient (the number observation within depth range) for three layers from the adjusted/new product and MEDATLAS vertical climatological profiles (called here Medar). Regions are defined according to Manca et al. (2004) (table 2S, Fig.2S)